

Finite Time Disentanglement Mediated by Plasmons for Different Waveguide Geometries



Seerat Javed
Regn.365134

A thesis submitted in partial fulfillment of the
requirements for the degree of **Master of Science**
in
Physics

Supervised by: Dr. Muzzamal Iqbal Shaukat
Co-Supervised by: Dr. Aeysha Khalique

Department of Physics

School of Natural Sciences
National University of Sciences and Technology
H-12, Islamabad, Pakistan
2023

THESIS ACCEPTANCE CERTIFICATE

Certified that final copy of MS thesis written by **Seerat Javed** (Registration No. **00000365134**), of **School of Natural Sciences** has been vetted by undersigned, found complete in all respects as per NUST statutes/regulations, is free of plagiarism, errors, and mistakes and is accepted as partial fulfillment for award of MS/M.Phil degree. It is further certified that necessary amendments as pointed out by GEC members and external examiner of the scholar have also been incorporated in the said thesis.

Signature: _____



Name of Supervisor: Dr. Muzzamal Iqbal Shaukat

Date: _____ 07-09-2023

Signature (HoD): _____



Date: _____ 07-09-2023


Signature (Dean/Principal): _____



Date: _____ 07.09.2023

National University of Sciences & Technology**MS THESIS WORK**

We hereby recommend that the dissertation prepared under our supervision by: Seerat Javed, Regn No. 00000365134 Titled: Finite Time Disentanglement Mediated by Plasmons for Different Waveguide Geometries be Accepted in partial fulfillment of the requirements for the award of **MS** degree.

Examination Committee Members1. Name: DR. TAJAMMAL HUSSAINSignature: 2. Name: DR. SAADI ISHAQSignature: Supervisor's Name DR. MUZZAMAL IQBAL SHAUKATSignature: Co Supervisor's Name DR. AEYSHA KHALIQUESignature: 

 Head of Department

07-09-2023
 Date
COUNTERSIGNEDDate: 07-09-2023

 Dean/Principal

Dedication

I dedicate my thesis to my parents for their love, support and encouragement throughout my education. Without their love and assistance, this work would not be possible.

Acknowledgements

First I would thank Allah, the Almighty for His blessings to complete my research work. Secondly, I would like to acknowledge and give my warmest thanks to my supervisor Dr. Muzzamal Iqbal Shaukat. His mentorship, patience and humble approach makes it possible to complete my work. I am extremely grateful for his invaluable advice and guidance through all the stages of my research work.

I would also like to thank my best friend Ansha Tayyab who always motivated me to complete the research tasks. Her help and company throughout my master degree was a constant support for me.

I also thank my family for encouraging me to achieve my academic goals. I specifically thank my brother who supports me throughout both financially and emotionally. Lastly, I would like to thank the administration of department for providing the learning environment and to all my extended friends for their help.

Abstract

In this thesis, entanglement dynamics of two distant qubits placed at a height h from plasmonic waveguide are investigated. For this purpose, two waveguide geometries are considered (i) cylindrical nanowire and (ii) V-shaped channel. To see the evolution of the system, Markovian master equation approach is used and density matrix elements are extracted. Entanglement generation is evaluated for ideal plasmonic waveguide and realistic channel waveguide. The influence of decay rates and coupling parameters on entanglement dynamics is analyzed. Moreover, entanglement sudden death is examined at specific qubit-qubit separation for different initial states. At later time, entanglement rebirth is observed and dark period is estimated for both geometries. It is noticed that the cylindrical geometry shows lesser dark period as compared to the V-shaped channel and the revival of entanglement is much more significant in perior waveguide geometry as compared to the lateral. Further, superdense coding as an application of quantum entanglement is also examined for certain initial states and it is observed that the optimal time of dense coding capacity is greater for the case of cylindrical geometry as compared to V-shaped channel.

Contents

List of Abbreviations	viii
List of figures	viii
1 Introduction	1
1.1 History	1
1.2 Motivation	4
1.3 Objectives and achievements	5
1.4 Structure of the Thesis	6
2 Fundamental Concepts	7
2.1 Qubit	7
2.2 Bloch sphere	8
2.3 Quantum states	10
2.3.1 Entangled state	11
2.3.2 Bell states	12
2.4 Density matrix	15
2.4.1 Pure state	16
2.4.2 Mixed state	17
2.5 Plasmonic waveguide	18
2.6 Concurrence	19
2.7 Decoherence	21

2.8	Entanglement sudden death	22
2.9	Superdense coding	23
3	Entanglement Generation	25
3.1	Model	25
3.2	Two-qubit entanglement dynamics	26
3.2.1	Master equation	27
3.2.2	Decay rates	33
3.3	Entanglement generation	34
4	Entanglement sudden death	36
4.1	Entanglement sudden death and revival	36
4.1.1	Entangled State	36
4.1.2	Mixed state	40
4.1.3	Werner State	41
4.1.4	Maximally non local mixed state	43
4.1.5	Maximally entangled mixed state	44
4.2	Superdense coding	46
4.2.1	Entangled state	47
4.2.2	Werner state	49
4.2.3	Maximally non-local mixed state	50
4.2.4	Maximally entangled mixed state	51
5	Result and discussion	53
	Bibliography	55

List of Abbreviations

EPR	Einstein–Podolsky–Rosen
ESD	Entanglement Sudden Death
EM	Electromagnetic
MNMS	Maximally Non-local Mixed State
MEMS	Maximally Entangled Mixed State
PW	Plasmonic Waveguide
QSDC	Quantum Superdense Coding
SDC	Superdense Coding

List of Figures

2.1	The Bloch sphere representation of a qubit state.	9
2.2	A vector representation of two system(qubits) variables	13
3.1	Two distant qubits q_1 and q_2 placed at height h from a waveguide.	26
3.2	(Color Online)Variation of concurrence and state populations (a) Ideal PW with $\beta = 1$ and $l = \infty$ (b) V-shaped channel. . .	35
4.1	(Color online) Variation of $C(t)$ for initial entangled state $ \Psi\rangle$ at $d \simeq h$ for (a) cylinder and (b) channel.	37
4.2	(Color online) Variation of $C(t)$ for initial entangled state $ \Psi\rangle$ at $a = 3/5$ and $d \simeq 5h/2$ for (a) cylinder and (b) channel . . .	38
4.3	(Color online) Variation of $C(t)$ for limiting case with $d \simeq h$ for (a) cylinder and (b) channel	39
4.4	(Color online)Variation of $C(t)$ for mixed state $ \Psi\rangle$ at $d \simeq 5h/2$ for (a) cylinder and (b) channel.	41
4.5	(Color online) Variation of $C(t)$ for initial state $ \Psi_i\rangle$ at $d \simeq$ $5h/2$ for (a) cylinder and (b) channel.	42
4.6	(Color online) Variation of a concurrence as function of dimen- sionless time parameter (γt) for two photon coherence MNMSs at $d \simeq 5h/2$ for (a) cylinder and (b) channel.	44
4.7	(Color online) Variation of a concurrence as function of dimen- sionless time parameter (γt) for two photon coherence MEMSs at $d \simeq 5h/2$ for (a) cylinder (b) channel.	45

4.8	(Color online) Schematic representation of information transfer between sender and receiver.	46
4.9	(Color online) Time variation of a χ for entangled state at $d \simeq 5h/2$ for (a) cylinder (b) channel.	48
4.10	(Color online) Time variation of a χ for werner state at $d \simeq 5h/2$ for (a) cylinder (b) channel.	49
4.11	(Color online) Time variation of a χ for MNMS at $d \simeq 5h/2$ for (a) cylinder (b) channel.	51
4.12	(Color online) Time variation of a χ for MEMS at $d \simeq 5h/2$ for (a) cylinder (b) channel.	52

Chapter 1

Introduction

1.1 History

A brief historical review of quantum mechanics, quantum optics and quantum information is done here. In scientific theories, quantum mechanics is the most successful and mysterious field. It is the basis of quantum computation and information. It was developed over a marvellous period from 1900 to 1920s. At the start of the twentieth century, physics was mainly comprised of classical mechanics, the concepts of thermodynamics and electromagnetism. Following the twentieth century, classical physics was desperately challenged as Einstein's relativistic theory showed the inconsistency of classical mechanics for the objects approaching speed of light. Moreover, classical physics failed in providing the proper explanation of phenomena like blackbody radiation, the photoelectric effect etc. to the level of atomic and subatomic structures. At nano-scale classical physics is not valid. After that there is a need to invoke new ideas outside this bound.

The first development proposed by Max Planck in 1900 gives the concept of energy quantization [1]. In 1905 following the Planck's idea of quantization, Einstein described that light itself is made up of discrete energy, called photons, each of energy hf where f is the light's frequency. Einstein's concept of photon gave the accurate explanation of the photoelectric effect. Another breakthrough occurs in 1919 when a model of hydrogen atom was proposed by

Bohr [2]. It was introduced after the Rutherford's discovery of atomic nucleus in 1911 Bohr proclaimed that the atoms can only be found in discrete energy states and interaction of atom with radiations took place in form of quanta of energy. In 1923 Compton confirms that X-rays photons behave like particles by scattering them with electrons [3]. This chain of progress by Einstein, Planck and Compton gave the theoretical and experimental confirmation of the particle nature of wave at microscopic scale. de-Broglie presented that not only radiations display wave-particle duality but it is the characteristic of metal itself. Davisson and Germer in 1927 [4] gives the experimental confirmation of this behaviour using electrons. They unveiled that the interference pattern (a property of waves) can also be obtained with material particles like electrons. The hydrogen's model was criticized for lacking theoretical information although it coincides well with experimental spectroscopy. The quantization of energy and the postulates endorsed by Bohr were quite unexpected and do not follow the principles of physics.

The dissatisfaction of Planck's and Bohr's models had provoked Heisenberg and Schrödinger to search for new ideas. By the end of 1925 their efforts paid off. Heisenberg, Schrödinger and Dirac laid the foundations of quantum mechanics in an surprisingly short period from 1925 to 1926 [5]. Representation, unitary transformation, quantum-state evolution, perturbation theory etc. all are given by them. There were two formalism of quantum mechanics, one is the matrix mechanics developed by Heisenberg and other is the wave mechanics by Schrödinger [6]. The matrix mechanics describes the structure of atoms inspired from Planck's idea of quantization and Bohr's concept of hydrogen atom. The Heisenberg stated the idea that systems are bound to follow the quantization of energy. To describe the dynamics of microscopic systems, he introduced the notion of matrices for analysis of eigen value problem. The second formalism (wave mechanics) is the abstraction of the de Broglie postulate. It states that the dynamics of microscopic systems is solved by using wave mechanics given by Schrödinger. Instead of

using matrix formalism, Schrödinger used the differential equation to analyse the system dynamics. The idea of intrinsic probabilistic nature of wave mechanics given by Max Born in 1927 allowed the fully quantum treatment of interference. Heisenberg's and Schrödinger's formalisms were shown to be equivalent. Later on Dirac proposed the ket-bra formalism of quantum states [7]. In continuous basis ket-bra formalism gives back Schrödinger's wave mechanics while in discrete basis it returns to Heisenberg's matrix mechanics. Dirac developed an equation in 1928 by combining special relativity with quantum mechanics called the Dirac's equation, which describes the motion of electrons. Fermi and Dirac being the pioneers of quantum mechanics addressed the quantization of light interacting with an atom. Reviews of Modern Physics article in the 1930s by Fermi's summarizes what was known at that time within the context of non relativistic quantum electrodynamics in the Coulomb gauge.

Einstein continued the study of nature of quantum mechanics and in 1935 with Boris Podolsky and Nathan Rosen published a remarkable work in which quantum correlations are stated. They found that when two particles have been strongly related, they share a single state. Measurement on one particle will influence the other even though they are far apart. This work is later known as EPR paradox [8] because of the three names on the paper. Bell demonstrated the upper limit for the strength of quantum correlations seen in Bell's inequality and showed that for certain entangled systems this limit is violated. The experimental breakthrough came in with the presentation of an apparatus in 1967 whose generated photons were seen to be entangled. This was the first case of entangled light [9]. Afterwards, quantum optics emerges as a separate subject. Researchers start investigating the coherence in light matter interaction with the development in theory of photon statistics. Quasi-probabilities developed much earlier by Wigner and others are used to describe the behaviour of light in free space. Resonant interactions and coherent transients led to the beginning of quantum optics after which

we were able to study the dynamics of single atom interacting with light. The study of single atom interacting with single mode electromagnetic field is achieved with the efforts of researchers by the end of 1980 [10]. An atom can coherently exchange excitation with field which result in loss of coherence known as decoherence through dissipative part of system. This is the elementary unit of quantum optics.

The information processing in quantum leads to the quantum cryptography and quantum computation which developed vigorously in recent years by Feymann, Deutsch, Bennett and others. In 1984, the discovery of quantum key protocols opens the path for quantum communication. These includes BB84 protocol by Charles H. Bennett and Gilles Brassard [11] and E91 by Artur Ekert [12]. Bell's work has a strong impact in these communication resources. For the proof of security, violation of Bell's inequality is used in E91 protocol. In 2022, Nabal Prize was also awarded "for experiments with entangled photons, establishing the violation of Bell inequalities and pioneering quantum information science" to Aspect, Clauser, and Anton Zeilinger [13].

1.2 Motivation

Quantum entanglement is turning up as an important aspect in field on quantum computing and information. In recent year, Nobel Prize was also awarded " for experiments with entangled photons, establishing the violation of Bell inequalities and pioneering quantum information science". The motivation behind this thesis is the necessity of entanglement for the complete deployment of quantum computing. It is a sort of computational multiplier for qubits. As we go on increasing the number of entangled qubits, the ability of the system to make calculations grows exponentially. Therefore, it is crucial to understand the phenomenon of early stage disentanglement often called entanglement sudden death (ESD) to analyze the dynamics of a sys-

tem. Entanglement is considered not to suffer from decoherence over a long period of time. But it is seen that due to some unavoidable noises, entanglement decay to zero in a finite time. Moreover, dense coding capacity being the application of entanglement is the important feature in quantum information. Therefore, it will be beneficial to see the evolution of dense coding capacity with time to analyze the quantum system.

1.3 Objectives and achievements

The objective of this thesis is to review the generation of entanglement and analyze the phenomenon of early stage disentanglement (ESD) of two qubits system mediated by plasmonic waveguide for different initial states. In addition to this, time variation of dense coding capacity is also examined as an application of entanglement. For this objective, two different waveguide geometries are studied i.e. cylindrical nanowire and V-shaped channel. Master equation approach is used to see the time evolution of density matrix elements. Moreover, entanglement rebirth or revival is noticed at later time for different initial states. Dark period is estimated for both geometries.

It is observed that the characteristics of the entanglement sudden birth are different for both geometries. It is worth to see the entanglement rebirth for all initial coherence values for the case of maximally entangled mixed state. The dark period of cylindrical geometry is found to be less than the V-shaped channel in wake of collective damping term. Moreover, dense coding capacity is analyzed for both geometries by considering different initial states. The optimal time of cylindrical geometry is found to be greater than the V-shaped channel. It is seen that dense coding capacity have maximum possible value for maximally entangled state.

1.4 Structure of the Thesis

The rest of the thesis is structured into four chapters. In 2nd chapter the fundamental concepts necessary to understand the quantum system are explained. Starting from a qubit (a basic building block of quantum information), Bloch sphere and quantum states are elaborated. In this chapter, representation of quantum state is shown, moreover a difference of pure and mixed state is also discussed. The phenomenon of entanglement is analyzed by studying the entangled state and Bell states. The basic structure of plasmonic waveguide is explained. The phenomenon of measurement of entanglement and the process of decoherence is studied. How entanglement decay to zero in a finite time which is the main subject of thesis is also discussed in this chapter.

In chapter 3 the physical model under consideration is explained. The dynamics of two qubits entanglement are analyzed and master equation is derived. Density matrix elements are examined and coupling parameters are reviewed. The generation of entanglement for ideal PW and realistic PW is compared.

In the fourth chapter, entanglement sudden death for the two qubits system mediated by plasmonic waveguide is investigated. Two geometries are considered for this purpose i.e. cylindrical nanowire and V-shaped channel. Death and revival time is examined and dark period is estimated for different initial states. On the basis of which both geometries are compared. Furthermore, dense coding capacity is also for examined for different initial states as an application of an entanglement. Lastly, all the results are concluded and discussed.

Chapter 2

Fundamental Concepts

2.1 Qubit

Qubit in quantum system is used as a basic source of information. A digital computer stores and transports information in form of bits. A bit is anything that have two distinct positioning one represented by 0 and other by 1. For example, a bulb can be on or off or the coin with head and tail, there is no intermediate situation. In communication, bits are represented by either the absence or presence of electrical signal carrying the value 0 or 1 respectively. Quantum bit is made up of quantum system such as photon or electron. Quantum bit can also exist in superposition state and even be entangled to other quantum bits whereas classical bit can have only two distinct configurations. When a particle is used as a qubit, it is kept under controlled environment. The superposition property of a quantum bit make it possible for quantum computers to be in more than one states at once. The number of states increases as 2^n , where n is the number of qubits.

Qubit is basically a two level quantum system whose basis states are generally represented as $|0\rangle$ and $|1\rangle$ or as a linear combination of both [14]. Generally, if we talk about the basis states of qubit, we are considering z-basis as computational basis which are represented in state vectors as:

$$|0\rangle = \begin{pmatrix} 1 \\ 0 \end{pmatrix}, \quad |1\rangle = \begin{pmatrix} 0 \\ 1 \end{pmatrix}.$$

A single qubit state is generally given as $\psi = a|0\rangle + b|1\rangle$, with amplitude a and b which can be normalized as $|a|^2 + |b|^2 = 1$

2.2 Bloch sphere

The field of quantum have unique applications in physics. Most of the problem solving techniques are addressed in quantum computing. The classical bit can hold a value of either 0 or 1. However, in today's world all magnificence of quantum computing lies in *quantum bit* or *qubit* which just not represent the 0 or 1 but an infinite array of their combinations known as superposition. We are now capable of sending a large amount of data as the superposition of 0 and 1. But the question is how does a quantum state look like? Realising the nature at such microscopic level is always remained a challenge for scientists. Mathematical and computing power is used to tackle this mystery. In quantum mechanics and quantum computing, Bloch sphere is the physical representation of quantum states of a two level system named after the physicist Felix Bloch. Each qubit(a two level system) is represented by a vector on a Bloch sphere [15]. Fig. 2.1 represents qubit state on a surface of a Bloch sphere, here $|+\rangle = \frac{1}{\sqrt{2}}(|0\rangle + |1\rangle)$, $|-\rangle = \frac{1}{\sqrt{2}}(|0\rangle - |1\rangle)$, $|+\iota\rangle = \frac{1}{\sqrt{2}}(|0\rangle + \iota|1\rangle)$ and $|-\iota\rangle = \frac{1}{\sqrt{2}}(|0\rangle - \iota|1\rangle)$. Researchers can utilize various states within the sphere to their advantage. Each vector is characterized by two basis: θ and ϕ . Here θ is the angle between vector and z-axis while ϕ is the angle between vector and positive x-axis. All possible vectors can be achieved by realizing θ and ϕ . The qubit state can be given as

$$\hat{n}(n_x, n_y, n_z) = (\cos\phi\sin\theta, \sin\phi\sin\theta, \cos\theta), \quad (2.1)$$

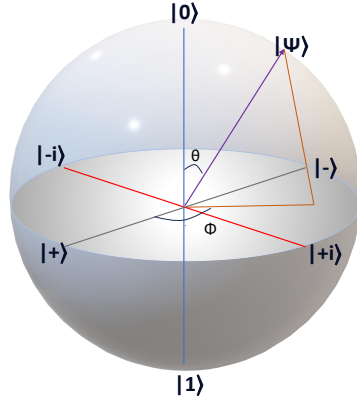


Figure 2.1: The Bloch sphere representation of a qubit state.

where \hat{n} is the Bloch vector. Consider a generic state, $|\psi\rangle = \cos(\frac{\theta}{2}) + e^{i\phi}\sin(\frac{\theta}{2})$ also written as

$$|\psi\rangle = \begin{pmatrix} \cos(\frac{\theta}{2}) \\ e^{i\phi}\sin(\frac{\theta}{2}) \end{pmatrix}, \quad (2.2)$$

different values of θ and ϕ leads to different states represented by different points on Bloch sphere. To determine the state of a qubit we should know either θ and ϕ or Bloch vector \hat{n} .

A	$\theta = 0, \phi = 0$	$ A\rangle = \begin{pmatrix} 1 \\ 0 \end{pmatrix}$
B	$\theta = \pi, \phi = 0$	$ B\rangle = \begin{pmatrix} 0 \\ 1 \end{pmatrix}$
C	$\theta = \pi/2, \phi = \pi$	$ C\rangle = \frac{1}{\sqrt{2}} \begin{pmatrix} 1 \\ -1 \end{pmatrix}$
D	$\theta = \pi/2, \phi = \pi/2$	$ D\rangle = \frac{1}{\sqrt{2}} \begin{pmatrix} 1 \\ i \end{pmatrix}$
E	$\theta = \pi/2, \phi = -\pi/2$	$ E\rangle = \frac{1}{\sqrt{2}} \begin{pmatrix} 1 \\ -i \end{pmatrix}$

From \hat{n} , we can write $n_x = \cos\phi\sin\theta$, $n_y = \sin\phi\sin\theta$, $n_z = \cos\theta$

$$\begin{aligned}\cos^2(\theta/2) &= \frac{1 + \cos\theta}{2}, \\ \cos(\theta/2) &= \sqrt{\frac{1 + n_z}{2}},\end{aligned}\tag{2.3}$$

$$\begin{aligned}e^{i\phi}\sin\left(\frac{\theta}{2}\right) &= \frac{e^{i\phi}\sin\frac{\theta}{2}\cos\frac{\theta}{2}}{\cos\frac{\theta}{2}} = \frac{e^{i\phi}\sin\theta}{2\cos\frac{\theta}{2}}, \\ &= \frac{1}{2\cos\frac{\theta}{2}}(\sin\theta\cos\phi + i\sin\theta\sin\phi),\end{aligned}\tag{2.4}$$

using Eq. (2.3), n_x and n_y we get

$$e^{i\phi}\sin\left(\frac{\theta}{2}\right) = \frac{n_x + in_y}{\sqrt{2(1 + n_z)}}.\tag{2.5}$$

Substituting Eq.(2.3) and Eq. (2.5) in Eq.(2.2) we get the state of a qubit in Bloch vectors representation

$$|\psi\rangle = \begin{pmatrix} \sqrt{\frac{1 + n_z}{2}} \\ \frac{n_x + in_y}{\sqrt{2(1 + n_z)}} \end{pmatrix}.\tag{2.6}$$

2.3 Quantum states

Quantum state is used to define the quantum system mathematically. States in classical mechanics are the one from which quantum states turn up. Any dynamical state in classical mechanics is defined by the real values at each point. For example, to represent a state of a ball there is need to define its position and velocity. The time evolution of values occur under the equation of motion but remained determined. While values from quantum states are complex number, quantized and provide a probability distribution as an outcome for a system. In quantum, position and momentum is defined but can not be measured simultaneously. This is recapitulated in uncertainty principle defined by Heisenberg [16] which states that if the position and

momentum are measured simultaneously then

$$\Delta x \cdot \Delta p \geq \frac{\hbar}{2}. \quad (2.7)$$

There are different ways to define a quantum state based on the kinds of problems or systems. These are classified into two general categories: wave functions which describes the quantum system with position or momentum variables and vector quantum states. These two categories further divide the system into pure and mixed state or into coherent and incoherent states.

Measurement is a macroscopic operation which filters the state when performed on a quantum state. In quantum, measurement is the manipulation of a physical system to yield the numerical value. Therefore, measurement prepares quantum states for experiments. When performed on states, it may alter the state and redefine it hence known as incompatible measurement.

2.3.1 Entangled state

Quantum entanglement is the most fascinating phenomenon in nature. This feature was first recognized by Einstein, Podolsky and Rosen (EPR) in 1935. This phenomenon occurs when a group of particles share spatial proximity in such a way that the quantum state of each particle can not be described independently of the other even when they are far apart. Entanglement has many useful applications including quantum cryptography, quantum teleportation and quantum dense coding.

In an entangled system, quantum states can not be defined as a product of its local constituents [17]. The state of such system is defined as a superposition of local constituents. Consider two systems X and Y with Hilbert space H_X and H_Y , the Hilbert space of composite system will be the tensor product of both Hilbert spaces:

$$H_{XY} = H_X \otimes H_Y. \quad (2.8)$$

If the individual systems are in state ψ_X and ψ_Y respectively, then the state of composite system is given as:

$$\psi_{XY} = \psi_X \otimes \psi_Y. \quad (2.9)$$

The states of the system that can be expressed as Eq. (2.9) or simply can be written as tensor product are known as separable states. The states that are not separable are called entangled states. Now let $|i_X\rangle$ are the basis for system X and $|i_Y\rangle$ for system Y, the simplest state can be written as:

$$\psi_{XY} = \sum_{i,j} C_{ij} |i_X\rangle \otimes |j_Y\rangle. \quad (2.10)$$

In this equation if C_i^X and C_j^Y are given such that $C_{ij} = C_i^X C_j^Y$, the state is separable while if $C_{ij} \neq C_i^X C_j^Y$ the state is inseparable called an entangled state. Consider the basis vectors $\{|0\rangle_X, |1\rangle_X\}$ and $\{|0\rangle_Y, |1\rangle_Y\}$ for H_X and H_Y respectively, the entangled state is given as: $\frac{1}{\sqrt{2}}(|00\rangle_{XY} + |11\rangle_{XY})$, hence it is not possible to write the either system explicitly in form of pure state. In this way, the given systems are entangled.

2.3.2 Bell states

Bell states are the class of maximally entangled states. These are the linear combination of two states $|0\rangle$ and $|1\rangle$. These are

$$\begin{aligned} |\phi^+\rangle &= \frac{1}{\sqrt{2}}(|00\rangle + |11\rangle), \\ |\phi^-\rangle &= \frac{1}{\sqrt{2}}(|00\rangle - |11\rangle), \\ |\psi^+\rangle &= \frac{1}{\sqrt{2}}(|01\rangle + |10\rangle), \\ |\psi^-\rangle &= \frac{1}{\sqrt{2}}(|01\rangle - |10\rangle). \end{aligned} \quad (2.11)$$

These states obey the general conditions required for every basis set that is these are orthogonal and linearly independent. Thus basis set is written as

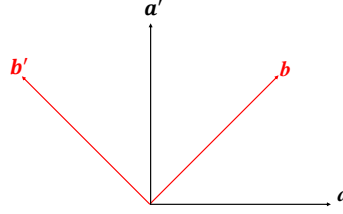


Figure 2.2: A vector representation of two system (qubits) variables

$B = \{|\phi^+\rangle, |\phi^-\rangle, |\psi^+\rangle, |\psi^-\rangle\}$. Bell defines mathematical prove of Einstein ambiguity by introducing Bell inequalities. Consider a two qubit system, a and a' are variable of one system whereas b and b' are of other (see Fig. 2.2). $a = \pm 1$ and $a' = \pm 1$ are two possible measurement outcome of one qubit whereas $b = \pm 1$ and $b' = \pm 1$ are possible results of measurement on second qubit. The combination of joint result can be written as,

$$\begin{aligned} C &= ab - ab' + a'b + a'b', \\ &= (a + a')b + (-a + a')b', \\ &= \pm 2. \end{aligned}$$

This correlation holds because either $a = a'$ or $a = -a'$, in first case second term vanishes while in second case first term vanishes.

$$\langle C \rangle = |\langle ab \rangle - \langle ab' \rangle + \langle a'b \rangle + \langle a'b' \rangle| \leq 2. \quad (2.12)$$

Bell inequality [18] involves the Bell operators a, a', b, b' with sigma σ because these operators have ± 1 eigen values.

$$\hat{a} = \vec{\sigma}.a, \hat{b} = \vec{\sigma}.b, \hat{a}' = \vec{\sigma}.a', \hat{b}' = \vec{\sigma}.b'. \quad (2.13)$$

Bell states violate Bell inequality to its maximum. Let consider a Bell state $|\psi_{-}\rangle$,

$$\begin{aligned}
\langle ab \rangle &= \langle \psi_{-} | \hat{a} \hat{b} | \psi_{-} \rangle, \\
&= \langle \psi_{-} | \sigma^A \cdot a \otimes \sigma^B \cdot b | \psi_{-} \rangle, \\
&= \langle \psi_{-} | \sum_i \sigma_i^A \cdot a_i \sum_j \sigma_j^B \cdot b_j | \psi_{-} \rangle, \\
&= \sum_i \sum_j a_i b_j \langle \psi_{-} | \sigma_i^A \otimes \sigma_j^B | \psi_{-} \rangle, \tag{2.14}
\end{aligned}$$

here operator with superscript A will operate on state of first qubit and the operator with superscript B will act on state of second qubit. After the operation of sigma operators on qubit states and simplifying Eq. (2.14) we will get

$$\begin{aligned}
\langle ab \rangle &= \sum_i \sum_j a_i b_j \delta_{ij} (-1), \\
&= - \sum_i a_i b_i, \\
&= -\cos(\theta), \tag{2.15}
\end{aligned}$$

hence after solving other terms of Eq. (2.12), we can write

$$\begin{aligned}
\langle ab \rangle &= -\cos(\theta)_{ab} = -\cos(\pi/4) = -1/\sqrt{2}, \\
\langle ab' \rangle &= -\cos(\theta)_{ab'} = -\cos(-3\pi/4) = 1/\sqrt{2}, \\
\langle a'b \rangle &= -\cos(\theta)_{a'b} = -\cos(\pi/4) = -1/\sqrt{2}, \\
\langle a'b' \rangle &= -\cos(\theta)_{a'b'} = -\cos(\pi/4) = -1/\sqrt{2}. \tag{2.16}
\end{aligned}$$

Substituting Eq. (2.16) in Eq. (2.12) will result in

$$\begin{aligned}
\langle C \rangle &= | -1/\sqrt{2} - 1/\sqrt{2} - 1/\sqrt{2} - 1/\sqrt{2} |, \\
\langle C \rangle &= 2\sqrt{2} > 2. \tag{2.17}
\end{aligned}$$

Therefore the Bell inequality is violated, as the Bell states violates the Bell inequality by maximum hence maximum inequality that can be violated by a quantum state is a factor of $\sqrt{2}$. Product state should not violate this correlation.

2.4 Density matrix

Density matrix was introduced by von Neumann to express the statistical concepts in quantum. In quantum mechanics, density matrix or density operator represents an alternate form of the quantum state of a physical system [19]. It is more powerful tool than the wave function for real experimentally generated quantum state. Moreover, decoherence and environmental effects can be accounted by the time evolution of the density matrix. Let suppose that the quantum system incorporates of $|\psi_m\rangle$ states then its density matrix is represented as a outer product of given states:

$$\rho(t) = \sum_m p_m |\psi_m\rangle \langle \psi_m|, \quad (2.18)$$

where $\sum_m p_m = 1$ Now if we specify the state as $|x\rangle$ then by taking $\langle x|\rho|x\rangle$, we can evaluate the probability of state x in the system. ρ plays a role of probability distribution in quantum system.

$$\langle x|\rho|x\rangle = \text{Tr}[x\rho], \quad (2.19)$$

where Tr refers to tracing over diagonal elements of the matrix. Wave functions and state vectors can only represent pure states but the density matrices can also describe the mixed states. Therefore, density operator is an important tool in dealing with mixed states. Some important properties of density operator are:

- Density operator ρ is Hermitian that is $\rho = \rho^\dagger$.
- ρ is positive semi-definite:

$$\begin{aligned} \langle \psi|\rho|\psi\rangle &= 0, \\ \langle \psi|\sum_m p_m |\psi_m\rangle \langle \psi_m|\psi\rangle &= \sum_m p_m \langle \psi|\psi_m\rangle \langle \psi_m|\psi\rangle \geq 0. \end{aligned}$$

- Trace of $\rho = 1$:

$$\begin{aligned}
\text{Tr}(\rho) &= \text{Tr}\left(\sum_m p_m |\psi_m\rangle \langle \psi_m|\right), \\
&= \sum_m p_m \text{Tr}(|\psi_m\rangle \langle \psi_m|), \\
&= \sum_m p_m \langle \psi_m | \psi_m \rangle, \\
&= 1.
\end{aligned}$$

- The joint density matrix of separable individual systems is the tensor product of the individual density matrices, $\rho_1 \otimes \rho_2 \otimes \rho_3 \otimes \dots \otimes \rho_n$.

A general density matrix of two qubit system is presented as

$$\begin{pmatrix}
\rho_{00} & \rho_{0+} & \rho_{0-} & \rho_{03} \\
\rho_{+0} & \rho_{++} & \rho_{+-} & \rho_{+3} \\
\rho_{-0} & \rho_{-+} & \rho_{--} & \rho_{-3} \\
\rho_{30} & \rho_{3+} & \rho_{3-} & \rho_{33}
\end{pmatrix}. \quad (2.20)$$

2.4.1 Pure state

Pure state is a state that can not be written as a combination of other quantum states. It can be presented by quantum ket as well as density matrix. The density operator of pure state is given as:

$$\rho = |\psi\rangle \langle \psi|, \quad (2.21)$$

where ψ is a quantum state. consider a pure state of form $|\psi\rangle = \frac{1}{\sqrt{2}}(|0\rangle + |1\rangle)$, now the density operator is presented as

$$\begin{aligned}
\rho &= \frac{(|0\rangle + |1\rangle)(\langle 0| + \langle 1|)}{2}, \\
&= \frac{|0\rangle \langle 0| + |0\rangle \langle 1| + |1\rangle \langle 0| + |1\rangle \langle 1|}{2}, \\
&= \frac{1}{2} \begin{pmatrix} 1 & 1 \\ 1 & 1 \end{pmatrix}.
\end{aligned}$$

For a pure state : $\text{Tr}(\rho) = \text{Tr}(\rho^2)$

$$\begin{aligned}\rho^2 &= \rho \cdot \rho, \\ &= |\psi\rangle \langle \psi| |\psi\rangle \langle \psi|, \\ &= |\psi\rangle \langle \psi|,\end{aligned}\tag{2.22}$$

as $\rho^2 = \rho$ hence $\text{Tr}(\rho) = \text{Tr}(\rho^2)$.

2.4.2 Mixed state

Mixed states are the probabilistic ensembles of the pure states and it can not be presented by a quantum ket. Therefore, density operator is utilized to describe the mixed states.

$$\rho = \sum_i p_i |\psi_i\rangle \langle \psi_i|,\tag{2.23}$$

where p_i is the probability amplitude of the corresponding wave function with $\sum_i p_i = 1$. Consider a wave function with 50% probability of $|0\rangle$ and other with 50% probability of $|1\rangle$ state

$$|\psi_1\rangle = \frac{1}{2} |0\rangle, |\psi_2\rangle = \frac{1}{2} |1\rangle.$$

Now the density matrix of above states

$$\begin{aligned}\rho &= p_1 |\psi_1\rangle \langle \psi_1| + p_2 |\psi_2\rangle \langle \psi_2|, \\ &= \frac{1}{2} |0\rangle \langle 0| + \frac{1}{2} |1\rangle \langle 1|, \\ &= \frac{1}{2} \begin{pmatrix} 1 & 0 \\ 0 & 1 \end{pmatrix}.\end{aligned}$$

For mixed state : $\text{Tr}(\rho^2) < \text{Tr}(\rho)$

$$\begin{aligned}
\rho^2 &= \rho \cdot \rho, \\
&= \sum_i p_i |\psi_i\rangle \langle \psi_i| \sum_j p_j |\psi_j\rangle \langle \psi_j|, \\
&= \sum_i \sum_j p_j p_i |\psi_i\rangle \langle \psi_i| |\psi_j\rangle \langle \psi_j|, \\
&= \sum_i \sum_j p_j p_i \delta_{ij} |\psi_i\rangle \langle \psi_j|, \\
&= \sum_i |p_i|^2 |\psi_i\rangle \langle \psi_i|. \tag{2.24}
\end{aligned}$$

Individual probability of each state is less than one, so its square will become much smaller hence $\rho^2 < \rho$ and $\text{Tr}(\rho^2) < \text{Tr}(\rho)$. It is inferred from density matrix of pure and mixed states that the off diagonal terms are the one making the difference between two states [20].

2.5 Plasmonic waveguide

Plasmon are the nanomaterials that can capture, confine and propagate the optical energy. The optical property of plasmon structures make them an interesting topic of research. A hybrid plasmonic waveguide is formed by separating a high refractive index material from metal surface by a gap. Plasmonic field is emerging due to the optical properties at a nanoscale. There are numerous waveguide structures that can confine energy at interface of metal and dielectric. The plasmonic structures that have muscular optical confinement includes metallic nanowires, V-shaped groove, metallic nanoparticles and wedges. These geometries have strong confinement only when operating near the frequency of surface plasmon ω_{pl} . Most of the plasmonic waveguides exhibit different behaviour in terms of propagation length and energy confinement. Propagation length l is the distance a mode travels before energy density decay into e^{-1} of its original value.

$$l = \frac{1}{2k_i}, \tag{2.25}$$

where wave vector imaginary part is represented by k_i as $k = k_r + ik_i$ [21]. Due to the unique properties of plasmonic structures, they have a range of applications in science and energy transfer. The field of quantum plasmonics is making its way towards optical devices for communication, computing applications and quantum sensor.

2.6 Concurrence

Entanglement being the weird phenomenon of quantum world is getting significance in recent years. It is necessary to quantify the entanglement. For both pure and mixed state of bipartite system there are ways of quantifying the entanglement. There is one way for pure states while three ways (including entanglement of formation, negativity and relative entropy of entanglement) for mixed states of such systems. In entanglement of formation [22], there is a simpler way of measuring the degree of entanglement of a system called concurrence. The concurrence of a quantum state is zero if the state is separable and one if the state is maximally entangled.

Consider a state of qubits as $|\Psi\rangle$ which is example of pure state.. The concurrence of the state will be defined as

$$C(\Psi) = |\langle \Psi | \tilde{\Psi} \rangle|, \quad (2.26)$$

where $\tilde{\Psi}$ is spin flip operation on Ψ and $|\tilde{\Psi}\rangle = (\sigma_y \otimes \sigma_y) |\Psi^*\rangle$. Here σ_y is the Pauli matrix $\begin{pmatrix} 0 & -i \\ i & 0 \end{pmatrix}$ and $|\Psi^*\rangle$ is the complex conjugate of $|\Psi\rangle$ in the basis $\{|00\rangle, |01\rangle, |10\rangle, |11\rangle\}$. The spin flip operation when applied takes the state of each qubit to the orthogonal state while the state is contrarily the other way around on the Bloch sphere in case of pure state. Hence the concurrence is zero for the pure state. Conversely, the maximally entangled state remains invariant under the spin flip operation resulting in maximum possible value of concurrence. If the qubit system is described by density operator rather than a state vector, then Pauli operator σ_y is applied on both sides of density

operator, hence the spin flip operator will be

$$\tilde{\rho} = (\sigma_y \otimes \sigma_y) \rho^* (\sigma_y \otimes \sigma_y). \quad (2.27)$$

The entanglement in case of pure state can be written as

$$E(\Psi) = \mathcal{E}(C(\Psi)),$$

where $C(\Psi)$ is the concurrence defined by Eq. (2.26) and \mathcal{E} is given as

$$\mathcal{E}(C) = -\frac{1 + \sqrt{1 - C^2}}{2} \log_2 \frac{1 + \sqrt{1 - C^2}}{2} - \frac{1 - \sqrt{1 - C^2}}{2} \log_2 \frac{1 - \sqrt{1 - C^2}}{2}. \quad (2.28)$$

The function $\mathcal{E}(C)$ ranges from 0 to 1 as the C goes from 0 to 1. Now for a mixed state of two qubits the entanglement is defined as

$$E(\rho) = \mathcal{E}(C(\rho)), \quad (2.29)$$

where $C(\rho)$ is defines as $C(\rho) = \max\{0, \zeta_1 - \zeta_2 - \zeta_3 - \zeta_4\}$, ζ_i being the non-negative real numbers are the eigen values in decreasing order of $R \equiv \sqrt{\sqrt{\rho} \tilde{\rho} \sqrt{\rho}}$, where R is the Hermitian matrix. If we consider an X-state, the general density matrix is given as:

$$\rho = \begin{pmatrix} \rho_{00} & 0 & 0 & \rho_{03} \\ 0 & \rho_{++} & \rho_{+-} & 0 \\ 0 & \rho_{-+} & \rho_{--} & 0 \\ \rho_{30} & 0 & 0 & \rho_{33} \end{pmatrix}, \quad (2.30)$$

with $\rho_{33} + \rho_{++} + \rho_{--} + \rho_{00} = 1$. The eigenvalues of matrix R are given by

$$\begin{aligned} \sqrt{\zeta_{1,2}(t)} &= |\rho_{03}(t)| \pm (\rho_{++}(t) + \rho_{--}(t)), \\ \sqrt{\zeta_{3,4}(t)} &= (\rho_{++}(t) - \rho_{--}(t)) \pm \sqrt{\rho_{00}(t)\rho_{33}(t)}. \end{aligned} \quad (2.31)$$

It is evident that for a particular value of matrix elements, there are two possibilities for the largest eigenvalue. Consequently, concurrence can be defined in two alternative ways

$$C(t) = \max\{0, C_1(t), C_2(t)\}, \quad (2.32)$$

where

$$\begin{aligned}
C_1(t) &= 2|\rho_{30}(t)| \\
&\quad - \sqrt{(\rho_{++}(t) + \rho_{--}(t))^2 - (\rho_{+-}(t) + \rho_{-+}(t))^2}, \\
C_2(t) &= \sqrt{(\rho_{++}(t) - \rho_{--}(t))^2 - (\rho_{+-}(t) - \rho_{-+}(t))^2} \\
&\quad - 2\sqrt{\rho_{33}(t)\rho_{00}(t)}. \tag{2.33}
\end{aligned}$$

$C_1(t)$ is sustainable for condition $\rho_{30}(0) \neq 0$ while for large symmetric and anti-symmetric initial populations, $C_2(t)$ is influential. $C_2(t)$ will arise only when imbalance of symmetric and anti-symmetric states population occurred.

2.7 Decoherence

Quantum coherence is brittle in a sense that when system come in contact with the noises, its coherence start decaying [23]. This is analyzed by the decay of off-diagonal terms in density matrix of the given state. When a quantum system comes in interaction with the environment, information is altered which is known as environmental decoherence. The environmental interaction suppresses the interference between states. The loss of a coherence is the hurdle in quantum communication tasks. Entangled states are the special forms of the coherent superposition of multipartite quantum states. These are considered important in quantum communication, quantum teleportation and superdense coding. Decoherence disentangles the states that is why it is crucial towards experimental realisation of quantum information processors.

Decoherence is mainly characterized into local and non-local decoherence which are important in understanding of qubits jointly controlled by common external sources such as electromagnetic field. The process of decoherence is gradual.

The one difference between decoherence and disentanglement [24] is that co-

herence of the composite system does not lost completely while entanglement decays completely after a characteristic time. Hence, in general entanglement is more brittle phenomenon as compared to the quantum coherence.

2.8 Entanglement sudden death

The dynamical behaviour of quantum system shows that the correlations such as entanglement between qubits can be degraded by environmental noises. If the correlations dies in finite time, it is known as early stage disentanglement also called entanglement sudden death (ESD) which has been deliberated by Yu and Elberly [25]. This decay of entanglement with time shared by two or more parties is unavoidable [26, 27, 28, 17]. Theoretical observations of two qubits entanglement shows that the degradation of entanglement does not always follow a half-life decay rule. It is possible for even a very weakly dissipative environment to degrade the entanglement of a system to zero in a finite time rather than by successive halves, which refers to entanglement sudden death.

A two part joint state is presented by a matrix called the density matrix ρ in quantum mechanics. In the presence of environmental noises, density matrix start changing with time. The degradation of entanglement is then tracked by the quantum mechanical phenomenon called concurrence which is written as Eq. (2.32). When concurrence is zero it means there is no entanglement and when it is one means entanglement is maximum. In case of a spontaneous emission, there is no environment involved except for the vacuum. There are still noisy effects due to the quantum fluctuations in vacuum which can not avoided. These noisy effect will decay the entanglement of atoms resulting in zero entanglement as their final fate.

Now the question arises that in how much time entanglement decays to zero? For this purpose we have considered different initial states in chapter.4 and time of ESD is observed for two different geometries.

2.9 Superdense coding

Quantum superdense coding (QSDC) or superdense coding (SDC) being an application of entanglement is widely used in quantum information science [29]. It can be beneficial in improving the capacity of quantum communication. It has been extensively studied both in theory and experiment. It allows us to transfer two classical bits of information only by sending one qubit with the assumption of pre-sharing a maximally entangled state (an Einstein-Podolsky-Rosen (EPR) state). Concisely two parties (sender and receiver) share the qubit in a Bell state. The sender performs Unitary operations and sends particles to the receiver. The receiver then can distinguish among states to obtain two classical bits of information. These protocols enhance channel capacity through entanglement between two users. SDC is a secure way of transferring information between two users through secret quantum coding. Suppose Alice and Bob are two parties, Alice wants to send a information (two bits) to Bob using qubit. For this purpose, an entangled state is prepared by third party called Charlie using a Bell circuit. In this way one qubit is sent to Alice and the other to Bob. After receiving the qubit, Alice now performs the desired operation on her qubit depending on the bits she wants to send to Bob. After Bob has received the entangled qubit, he performs suitable quantum gate and recover the information of two bit message after measurement. In all this protocol, Alice does not find a need to communicate to Bob which gate operation he should apply on qubit to get the correct bit information [30].

For example, let consider a Bell state (an entangled state) as $|\eta_+\rangle_{AB} = \frac{1}{\sqrt{2}}(|0\rangle_A \otimes |0\rangle_B + |1\rangle_A \otimes |1\rangle_B)$ also written as $|\eta_+\rangle_{AB} = \frac{1}{\sqrt{2}}(|0\rangle_A |0\rangle_B + |1\rangle_A |1\rangle_B)$ is sent to the Alice and Bob, subscript A corresponds to Alice and B to Bob. Now Alice will decide the coding depending on the message she wants to send. Alice can transform the entangled state into any of the four Bell states by performing the quantum gate. Let say, if Alice has to

send 00, then she will apply the identity quantum gate $I = \begin{pmatrix} 1 & 0 \\ 0 & 1 \end{pmatrix}$ on her qubit, hence the resulting state will remain unchanged. If Alice wants to send 01, 10, 11 bit then the gate operation will change to $I = \begin{pmatrix} 0 & 1 \\ 1 & 0 \end{pmatrix}$, $I = \begin{pmatrix} 1 & 0 \\ 0 & -1 \end{pmatrix}$ and $I = \begin{pmatrix} 0 & 1 \\ -1 & 0 \end{pmatrix}$ respectively. After performing one of these operations, Alice send entangled qubit to Bob through some channel. Bob then decodes the encoding sent by Alice. For this, Bob will perform CNOT unitary operation with A controlled and B as target qubit, then he will perform $H \otimes I$ operation on qubit A and by the resulting basis Bob will come to know the bit string Alice has sent. For example, if the entangled state of Alice was $\frac{1}{\sqrt{2}}(|10\rangle_{AB} + |01\rangle_{AB})$, which means Alice wants to send bit 01 then in the Bob's lab CNOT operation will change the previous state to $\frac{1}{\sqrt{2}}(|11\rangle_{AB} + |01\rangle_{AB})$. Now Hadamard H gate is applied only to A which will result in state $\frac{1}{2}((|0\rangle - |1\rangle) \otimes |1\rangle + (|0\rangle + |1\rangle) \otimes |1\rangle)$, for simplicity subscripts are removed. After simplification Bob will get $|01\rangle$ as an end result hence he knows that Alice wants to send 01 as two bit message.

Chapter 3

Entanglement Generation

In this chapter, generation of two qubit entanglement is reviewed for two different waveguide geometries. For this objective, first model of system is explained, then master equation is derived and evolution of density matrix elements is observed.

3.1 Model

The system under analysis is consists of two qubits placed at a horizontal distance d from each other and at height h from metallic waveguide. The qubit system is placed nearby metallic waveguide to enhance the electromagnetic (EM) interaction by 1-D plasmonic structures. Qubits will be treated as two level system with transition frequency ω_0 compatible to the emission wavelength $\lambda = 600\text{nm}$ see Fig. 3.1. Two different waveguide geometries are reviewed to check their influence, (i) cylindrical nanowire and (ii) V-shaped channel waveguide. To analyze the both geometries, their parameters are defined in such a way that propagation length (see section 2.5) is same for both. Plasmonic modes are responsible for qubit-qubit interaction in the model, identical propagation length will be meaningful in comparison of both geometries. The propagation length l is kept $1.7\mu\text{m}$. The metal considered is silver in this case.

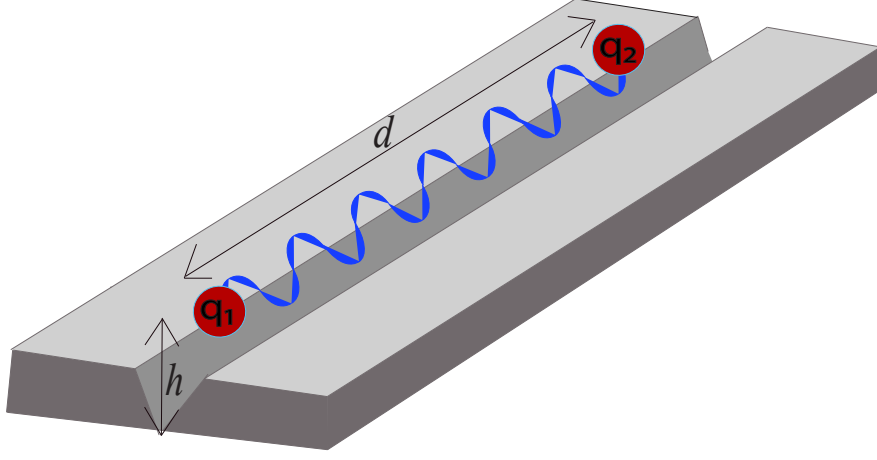


Figure 3.1: Two distant qubits q_1 and q_2 placed at height h from a waveguide.

3.2 Two-qubit entanglement dynamics

The entanglement dynamics of two level system are analyzed in this section. The interaction of the system with EM field mediated by plasmons can be illustrated by Green's tensor approach [31]. Thus all the parameters can be extracted from the classical Green's tensor that will describe the interaction between system and the environment. The Hamiltonian of the system is

$$\hat{H} = \hat{H}_0 + \hat{H}_I, \quad (3.1)$$

$$\begin{aligned} \hat{H} = & \int d^3R \int_0^\infty d\omega \hbar\omega \hat{b}^\dagger(\mathbf{R}, \omega) \hat{b}(\mathbf{R}, \omega) + \sum_{i=1,2} \hbar\omega_0 \hat{\sigma}_i^+ \hat{\sigma}_i^- \\ & + H_I. \end{aligned} \quad (3.2)$$

Where \mathbf{R} is the position, $\hat{\sigma}_i^-$ and $\hat{\sigma}_i^+$ are the lowering and raising operators of i -qubit respectively, \hat{b}^\dagger and \hat{b} are the bosonic fields playing the role of electromagnetic field and dielectric medium variables, ω_0 is the transition frequency and H_I is the Hamiltonian which is responsible for interaction between atoms and the electromagnetic field.

$$H_I = -i\hbar \sum_{\mathbf{k}} \sum_{i=1}^N [\tilde{\mu}_i \cdot \tilde{\mathbf{g}}_{\mathbf{k}} (\sigma_i^+ + \sigma_i^-) \hat{b}_{\mathbf{k}} - \text{H.c.}], \quad (3.3)$$

and EM operator is given as

$$\hat{E}(\mathbf{R}, \omega) = \iota \sqrt{\frac{\hbar}{\pi \epsilon_0}} \frac{\omega^2}{c^2} \int d^3 \mathbf{R}' \sqrt{\mathcal{E}_I(\mathbf{R}', \omega)} G(\mathbf{R}, \mathbf{R}', \omega) \hat{b}(\mathbf{R}', \omega). \quad (3.4)$$

Here $G(\mathbf{R}, \mathbf{R}', \omega)$ represents the Green's tensor [32, 33] which carries the EM interaction from spatial point \mathbf{R}' to \mathbf{R} and $\mathcal{E}(\mathbf{R}', \omega) = \mathcal{E}_r(\mathbf{R}', \omega) + i\mathcal{E}_I(\mathbf{R}', \omega)$ which is Kramers-Kronig consistent permittivity.

The transformation of Hamiltonian is given as

$$\begin{aligned} \hat{H}_I(t) &= e^{\iota \hat{H}_0 t} \hat{H}_I e^{-\iota \hat{H}_0 t}, \\ &= -\iota \hbar \sum_k \sum_{i=1}^N \{ \vec{\mu}_i \cdot \vec{g}_k \sigma_i^+ \hat{b}_k e^{-\iota(\omega_k - \omega_i)t} + \vec{\mu}_i \cdot \vec{g}_k \sigma_i^- \hat{b}_k e^{-\iota(\omega_k + \omega_i)t} - \text{H.c.} \}. \end{aligned} \quad (3.5)$$

$$(3.6)$$

Entanglement dynamics of the two qubits governed by their EM interaction can be described by reduced density matrix $\hat{\rho}$ of the corresponding system.

3.2.1 Master equation

Consider ρ_{qf} is the density matrix representing the statistical states of combined system. The system Hamiltonian variation with time in terms of a density operator is given as

$$\frac{\partial \hat{\rho}_{qf}}{\partial t} = \frac{1}{\iota \hbar} [\hat{H}, \hat{\rho}_{qf}]. \quad (3.7)$$

In interaction picture, Eq. (3.7) can be written as

$$\tilde{\rho}_{qf}(t) = e^{\iota \hat{H} t / \hbar} \hat{\rho}_{qf} e^{-\iota \hat{H} t / \hbar}. \quad (3.8)$$

The transformed density matrix should satisfy the Heisenberg's picture,

$$\frac{\partial \tilde{\rho}_{qf}(t)}{\partial t} = \frac{1}{\iota \hbar} [\hat{H}_I, \tilde{\rho}_{qf}], \quad (3.9)$$

$$\tilde{\rho}_{qf}(t) = \tilde{\rho}_{qf}(0) + \frac{1}{\iota \hbar} \int_0^t dt' [\hat{H}_I(t'), \tilde{\rho}_{qf}(t')], \quad (3.10)$$

where \hat{H}_I is the interaction Hamiltonian. Substituting Eq. (3.10) in right side of Eq. (3.9):

$$\begin{aligned}\frac{\partial \tilde{\rho}_{qf}(t)}{\partial t} &= \frac{1}{i\hbar} [\hat{H}_I, \tilde{\rho}_{qf}(0) + \frac{1}{i\hbar} \int_0^t dt' [\hat{H}_I(t'), \tilde{\rho}_{qf}(t')]], \\ &= \frac{1}{i\hbar} [\hat{H}_I, \tilde{\rho}_{qf}(0)] - \frac{1}{\hbar^2} \int_0^t dt' [\hat{H}_I, [\hat{H}_I(t'), \tilde{\rho}_{qf}(t')]],\end{aligned}\quad (3.11)$$

now taking trace over vacuum field variables and writing reduced density matrix of the qubit system $\hat{\rho}_q(t) = Tr_f \tilde{\rho}_{qf}(t)$,

$$\frac{\partial \hat{\rho}_q(t)}{\partial t} = \frac{1}{i\hbar} Tr_f [\hat{H}_I, \tilde{\rho}_{qf}(0)] - \frac{1}{\hbar^2} \int_0^t dt' Tr_f \{ [\hat{H}_I, [\hat{H}_I(t'), \tilde{\rho}_{qf}(t')]] \}.\quad (3.12)$$

Initial state is chosen so that the qubit system and the vacuum field have no correlation between them. This will allow us to factorize initial density operator of combined system as

$$\tilde{\rho}_{qf}(0) = \hat{\rho}_q(0) \hat{\rho}_f(0),\quad (3.13)$$

here $\hat{\rho}_f$ represents the density matrix of vacuum field. Now Born approximation [34] will be applied which means interaction between qubits and the EM field is weak and in field there is no back reaction on the system. Hence, in this approximation, state of vacuum do not move in time, so density operator $\tilde{\rho}_{qf}(t')$ of Eq. (3.12) results in

$$\tilde{\rho}_{qf}(t') = \hat{\rho}_q(t') \hat{\rho}_f(0).\quad (3.14)$$

After this approximation, changing the variable of time parameter $t' = t - \tau$ and simplifying

$$\begin{aligned}\frac{\partial \hat{\rho}(t)}{\partial t} &= \frac{1}{i\hbar} Tr_f [\hat{H}_I, \hat{\rho}_q(0) \hat{\rho}_f(0)], \\ &\quad - \frac{1}{\hbar^2} \int_0^t d\tau Tr_f \{ [\hat{H}_I(t), [\hat{H}_I(t - \tau), \hat{\rho}_q(t - \tau) \hat{\rho}_f(0)]] \}.\end{aligned}\quad (3.15)$$

After substituting $\hat{H}_I(t)$, we will see the dependence of density operator on correlation function of vacuum field operators. These correlations are given

as

$$\begin{aligned}
\text{Tr}_f[\hat{\rho}_f(0)\hat{b}_k] &= \text{Tr}_f[\hat{\rho}_f(0)\hat{b}_k^\dagger] = 0, \\
\text{Tr}_f[\hat{\rho}_f(0)\hat{b}_k\hat{b}_{k'}^\dagger] &= [|D(\omega_k)|^2 N(\omega_k) + 1]\delta^3(k - k')\delta_{ss'}, \\
\text{Tr}_f[\hat{\rho}_f(0)\hat{b}_k^\dagger\hat{b}_k] &= |D(\omega_k)|^2 N(\omega_k)\delta^3(k - k')\delta_{ss'}, \\
\text{Tr}_f[\hat{\rho}_f(0)\hat{b}_{k'}\hat{b}_k] &= D(\omega_k)^2 M(\omega_k)\delta^3(2k_s - k - k')\delta_{ss'}, \\
\text{Tr}_f[\hat{\rho}_f(0)\hat{b}_{k'}^\dagger\hat{b}_k^\dagger] &= D(\omega_k)^* M^*(\omega_k)\delta^3(2k_s - k - k')\delta_{ss'}.
\end{aligned} \tag{3.16}$$

Now changing the sum into integral

$$\sum_k \longrightarrow \frac{V}{(2\pi c)^3} \sum_{s=1}^2 \int_0^\infty d\omega_k \omega_k^2 \int d\Omega_k, \tag{3.17}$$

using the correlation functions from Eq. (3.16) and after applying rotating-wave approximation, the master equation will take the form as

$$\begin{aligned}
\frac{\partial \hat{\rho}}{\partial t} &= \sum_{i,n} \{ [\sigma_n^- \hat{X}_{in}(t, \tau), \sigma_i^+] + [\sigma_n^-, \hat{X}_{ni}^\dagger(t, \tau) \sigma_n^+] + [\sigma_n^+ \hat{Y}_{in}(t, \tau), \sigma_i^-] \\
&\quad + [\sigma_n^+, \hat{Y}_{ni}^\dagger(t, \tau) \sigma_n^-] + [\sigma_i^+ \hat{Z}_{in}(t, \tau), \sigma_n^+] + [\sigma_i^+, \hat{Z}_{in}(t, \tau) \sigma_n^+] \\
&\quad + [\sigma_i^- \hat{Z}_{in}^\dagger(t, \tau), \sigma_n^-] + [\sigma_i^-, \hat{Z}_{in}^\dagger(t, \tau) \sigma_n^-] \},
\end{aligned} \tag{3.18}$$

here the time operators are given as

$$\begin{aligned}
\hat{X}_{in} &= \frac{V}{(2\pi c)^3} \int d\omega_k \omega_k^2 e^{-i(\omega_i - \omega_n)t} \int d\Omega_k \sum_{s=1}^2 \zeta_{in}^-(t, \tau), \\
\hat{Y}_{in} &= \frac{V}{(2\pi c)^3} \int d\omega_k \omega_k^2 e^{i(\omega_i - \omega_n)t} \int d\Omega_k \sum_{s=1}^2 \zeta_{in}^+(t, \tau), \\
\hat{Z}_{in} &= \frac{V}{(2\pi c)^3} \int d\omega_k \omega_k (2\omega_s - \omega_k) e^{-i(2\omega_s - \omega_i - \omega_n)t} \int_{\Omega_s} d\Omega_k \sum_{s=1}^2 \zeta_{in}^M(t, \tau),
\end{aligned} \tag{3.19}$$

with

$$\begin{aligned}
\zeta_{in}^\pm(t, \tau) &= [|D(\omega_k)|^2 N(\omega_k) + 1][\mu_i \cdot g_k][\mu_n^* \cdot g_k^*] \int_0^t d\tau \hat{\rho}(t - \tau) e^{-i(\omega_k \pm \omega_n)\tau} \\
&\quad + [|D(\omega_k)|^2 N(\omega_k)][\mu_i^* \cdot g_k^*][\mu_n \cdot g_k] \int_0^t d\tau \hat{\rho}(t - \tau) e^{+i(\omega_k \mp \omega_n)\tau}, \\
\zeta_{in}^M(t, \tau) &= M(\omega_k) D^2(\omega_k) [\mu_i \cdot g_k][\mu_n \cdot g_k] \int_0^t d\tau \hat{\rho}(t - \tau) e^{+i(2\omega_s - \omega_k \mp \omega_n)\tau}.
\end{aligned} \tag{3.20}$$

The master Eq. (3.18) with parameters given in Eq. (3.19) and Eq. (3.20) is a general form of an integro-differential equation and can be simplified by using Markovian approximation. According to this approximation, the density operator hardly changes from $\hat{\rho}(t)$ over a time period τ . Therefore, by replacing $\hat{\rho}(t - \tau)$ by $\hat{\rho}(t)$ in Eq. (3.20). By extending the integral to infinity and performing integration over τ we get

$$\lim_{t \rightarrow \infty} \int_0^t d\tau \hat{\rho}(t - \tau) e^{\iota x t} \approx \hat{\rho}(t) \left[\pi \delta(x) + \iota \frac{P}{x} \right], \quad (3.21)$$

where P is the principle integral value. To carry out the integral over $d\Omega_k$ in Eq. (3.19) spherical representation is used for wave vector k and dipole moments are kept parallel of two level system, hence

$$k = |\vec{k}| [\sin\theta \cos\phi, \sin\theta \sin\phi, \cos\theta], \quad (3.22)$$

and orientation of atomic dipole can be taken as

$$\begin{aligned} \mu_i &= |\mu_i| [1, 0, 0], \\ \mu_n &= |\mu_n| [1, 0, 0], \end{aligned} \quad (3.23)$$

so with this choice of vectors and dipole moments, we obtain

$$\begin{aligned} \hat{X}_{in}(t, \tau) &= \{[1 + \hat{N}(\omega_s)] \left(\frac{1}{2} \gamma_{in} - \iota \Omega_{in}^- \right) + \iota \hat{N}(\omega_s) \Omega_{in}^+ \} \hat{\rho}(t) e^{-\iota(\omega_i - \omega_n)t}, \\ \hat{Y}_{in}(t, \tau) &= \{[\tilde{N}(\omega_s)] \left(\frac{1}{2} \gamma_{in} + \iota \Omega_{in}^- \right) - \iota [1 + \tilde{N}(\omega_s) \Omega_{in}^+] \} \hat{\rho}(t) e^{\iota(\omega_i - \omega_n)t}, \\ \hat{Z}_{in}(t, \tau) &= \tilde{M}(\omega_s) \left(\frac{1}{2} \gamma_{in} + \iota \Omega_{in}^M \right) \hat{\rho}(t) e^{-\iota(2\omega_s - \omega_i - \omega_n)t}, \end{aligned} \quad (3.24)$$

where

$$\begin{aligned} \tilde{N}(\omega_s) &= N(\omega_s) |D(\omega_s)|^2 \frac{1}{2} \left[1 - \frac{1}{4} (3 + \cos^2\theta) \cos\theta \right], \\ \tilde{M}(\omega_s) &= M(\omega_s) |D(\omega_s)|^2 \frac{1}{2} \left[1 - \frac{1}{4} (3 + \cos^2\theta) \cos\theta \right]. \end{aligned} \quad (3.25)$$

The parameter γ_{in} apperaing in Eq. (3.24) is emission rate when $i = n$ such that

$$\gamma_{ii} = \frac{\omega_i^3 \mu_i^2}{3\pi \mathcal{E}_0 c^3}, \quad (3.26)$$

and when $i \neq n$ is the collective spontaneous emission rate arises due to interaction between qubits through the EM field.

$$\gamma_{in} = \sqrt{\gamma_i \gamma_n J(kr)}, \quad (3.27)$$

here

$$J(kr) = \frac{3}{2} \left([1 - (\mu.r)^2] \frac{\sin(kr)}{kr} + [1 - 3(\mu.r)^2] \left[\frac{\cos(kr)^2}{kr} - \frac{\sin(kr)^3}{kr} \right] \right). \quad (3.28)$$

The remaining parameters of Eq. (3.24) are given as

$$\begin{aligned} \Omega_{in}^{\pm} &= P \frac{\sqrt{\gamma_i \gamma_n}}{2\pi \omega_0^3} \int_0^{\infty} \frac{\omega_k^3 J(\omega_k r/c)}{\omega_k \pm \omega_n} d\omega_k, \\ \Omega_{in}^M &= P \frac{\sqrt{\gamma_i \gamma_n}}{2\pi \omega_0^3} \int_0^{\infty} \frac{\omega_k^2 (2\omega_s - \omega_k) J(\omega_k r/c)}{2\omega_s - \omega_k - \omega_n} d\omega_k, \end{aligned} \quad (3.29)$$

Hence, the master equation with parameters of Eq. (3.24) is written as

$$\begin{aligned} \frac{\partial \hat{\rho}}{\partial t} &= -\frac{1}{2} \sum_{i,n=1}^N \gamma_{in} [1 + \tilde{N}(\omega_s)] (\hat{\rho} \sigma_i^+ \sigma_n^- + \sigma_i^+ \sigma_n^- \hat{\rho} - 2\sigma_n^- \hat{\rho} \sigma_i^+) \\ &\quad - \frac{1}{2} \sum_{i,n=1}^N \gamma_{in} \tilde{N}(\omega_s) (\hat{\rho} \sigma_i^- \sigma_n^+ + \sigma_i^- \sigma_n^+ \hat{\rho} - 2\sigma_n^+ \hat{\rho} \sigma_i^-) \\ &\quad + \frac{1}{2} \sum_{i,n=1}^N (\gamma_{in} + \iota \Omega_{in}^M) \tilde{M}(\omega_s) (\hat{\rho} \sigma_i^+ \sigma_n^+ + \sigma_i^+ \sigma_n^+ \hat{\rho} - 2\sigma_n^+ \hat{\rho} \sigma_i^+) \\ &\quad + \frac{1}{2} \sum_{i,n=1}^N (\gamma_{in} - \iota \Omega_{in}^M) \tilde{M}^*(\omega_s) (\hat{\rho} \sigma_i^- \sigma_n^- + \sigma_i^- \sigma_n^- \hat{\rho} - 2\sigma_n^- \hat{\rho} \sigma_i^-) \\ &\quad - \iota \sum_{i=1}^N (\omega_i + \delta_i) [\sigma_i^z, \hat{\rho}] - \iota \sum_{i \neq n}^N \Omega_{in} [\sigma_i^+ \sigma_n^-, \hat{\rho}], \end{aligned} \quad (3.30)$$

where δ_i is the lamb shift of atomic levels which depends on intensity given as

$$\delta_i = [2\tilde{N}(\omega_s) + 1](\Omega_{ii}^+ - \Omega_{ii}^-), \quad (3.31)$$

and vacuum induced coherent interaction between qubits is given as

$$\Omega_{in} = -(\Omega_{in}^+ + \Omega_{in}^-). \quad (3.32)$$

The final form of master equation is given by Eq. (3.30) which shows the dynamics of two interacting qubits. The interacting parameters γ_{in} and Ω_{in} modify the system. γ_{in} is the coupling between qubits due to the vacuum field and Ω_{in} is the coherent dipole-dipole interacting term. Here dipole-dipole interacting term plays the same role as Rabi frequency in atom-field interaction. In case of interaction of atom with ordinary vacuum, $\tilde{N}(\omega_s) = \tilde{M}(\omega_s) = 0$ the resulting equation will take the form

$$\frac{\partial \hat{\rho}}{\partial t} = -\frac{i}{\hbar}[\hat{H}_s, \hat{\rho}] - \frac{1}{2} \sum_{i,n} \gamma_{in} (\hat{\rho} \hat{\sigma}_i^+ \hat{\sigma}_n^- + \hat{\sigma}_i^+ \hat{\sigma}_n^- \hat{\rho} - 2\hat{\sigma}_n^- \hat{\rho} \hat{\sigma}_i^+), \quad (3.33)$$

where

$$\hat{H}_s = \sum_i \hbar(\omega_0 + \delta_i) \hat{\sigma}_i^+ \hat{\sigma}_i^- + \sum_{i \neq n} \hbar \Omega_{in} \hat{\sigma}_i^+ \hat{\sigma}_n^-. \quad (3.34)$$

Here δ_i is the Lamb shift due to the self electromagnetic association of qubits in existence of plasmonic waveguide, $\gamma_{11} = \gamma_{22} = \gamma$ is the spontaneous emission. The master equation is solved by employing the Dicke bases $|0\rangle = |g_1 g_2\rangle$, $|\pm\rangle = \frac{1}{\sqrt{2}}(|g_1 e_2\rangle \pm |e_1 g_2\rangle)$ and $|3\rangle = |e_1 e_2\rangle$ [35] to obtain the

density matrix elements given by

$$\begin{aligned}
\rho_{33}(t) &= e^{-2\gamma t} \rho_{33}(0), \\
\rho_{++}(t) &= e^{-(\gamma+\gamma_{12})t} \rho_{++}(0) \\
&\quad + \frac{\gamma + \gamma_{12}}{\gamma - \gamma_{12}} (e^{-(\gamma+\gamma_{12})t} - e^{-2\gamma t}) \rho_{33}(0), \\
\rho_{--}(t) &= e^{-(\gamma-\gamma_{12})t} \rho_{--}(0) \\
&\quad + \frac{\gamma - \gamma_{12}}{\gamma + \gamma_{12}} (e^{-(\gamma-\gamma_{12})t} - e^{-2\gamma t}) \rho_{33}(0), \\
\rho_{+-}(t) &= e^{-(\gamma-2i\Omega)t} \rho_{+-}(0), \\
\rho_{-+}(t) &= e^{-(\gamma+2i\Omega)t} \rho_{-+}(0),
\end{aligned} \tag{3.35}$$

along $\rho_{00}(t) = 1 - \rho_{33}(t) - \rho_{++}(t) - \rho_{--}(t)$.

3.2.2 Decay rates

Qubit-qubit interaction is mainly caused by plasmon and dipole couples mainly to plasmon mode. By using plasmonic contribution of Green's tensor, the dipole-dipole shift and decay rates are given as follows

$$\begin{aligned}
\Omega_{in} &= \frac{\gamma}{2} \beta e^{-d/2l} \sin(kd), \\
\gamma_{in} &= \gamma \beta e^{-d/2l} \cos(kd),
\end{aligned} \tag{3.36}$$

where l is the propagation length of plasmon, d is the qubit-qubit separation, k is the wave vector expressed as $k = 2\pi/\lambda_{pl}$. Beta factor β is the ratio of plasmon decay rate γ_{pl} and all the emissions coupled to plasmon $\beta = \gamma_{pl}/\gamma$. In both geometries, the orientation of qubits are set such that the β is maximum. For this purpose, h height of qubit from waveguide is kept 20nm and 150nm for cylinder and V-shaped channel respectively. The orientation of cylinder is set as vertical and for channel horizontal orientation is kept to maximize β . 417nm is chosen as operating wavelength for cylinder and 474nm for V-shaped channel. The corresponding β factor in accordance with these parameters is 0.6 and 0.9 for cylinder and channel respectively.

3.3 Entanglement generation

Consider two identical distant qubits. In this case, d is set equal to λ_{pl} . The position and orientation of PW is chosen in such a way to maximize the β factor. The system initial state is taken as $|10\rangle = |e_1g_2\rangle = \frac{1}{\sqrt{2}}(|+\rangle + |-\rangle)$, which is an unentangled state.

$$|e_1g_2\rangle \langle e_1g_2| = \frac{1}{2}(|+\rangle + |-\rangle)(\langle +| + \langle -|). \quad (3.37)$$

In this case the evolution is confined to $\{|0\rangle, |+\rangle, |-\rangle\}$ and hence the density matrix elements reduced to

$$\begin{aligned} \rho_{++}(t) &= e^{-(\gamma+\gamma_{12})t} \rho_{++}(0), \\ \rho_{--}(t) &= e^{-(\gamma-\gamma_{12})t} \rho_{--}(0), \\ \rho_{+-}(t) &= e^{-(\gamma-2i\Omega)t} \rho_{+-}(0), \\ \rho_{-+}(t) &= e^{-(\gamma+2i\Omega)t} \rho_{-+}(0), \end{aligned} \quad (3.38)$$

along $\rho_{00}(t) = 1 - \rho_{++}(t) - \rho_{--}(t)$.

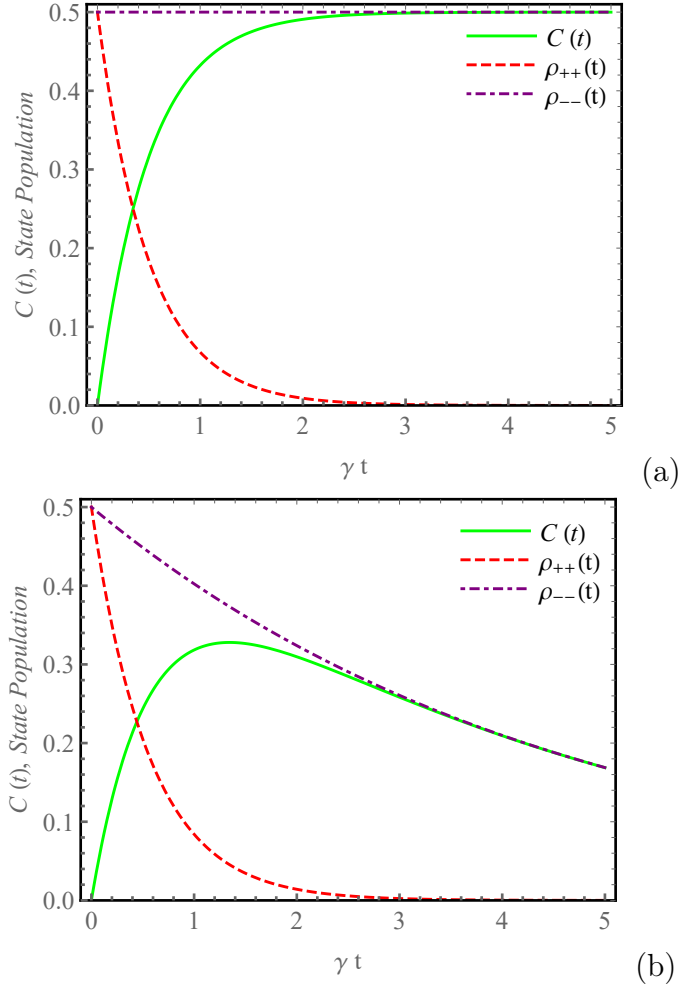


Figure 3.2: (Color Online) Variation of concurrence and state populations (a) Ideal PW with $\beta = 1$ and $l = \infty$ (b) V-shaped channel.

The concurrence (Eq.(2.33)) and populations ($\rho_{++}(t), \rho_{--}(t)$) are plotted in Fig. 3.2. For an ideal PW case, it is seen that entanglement grows with time upto $C(t) = 0.5$ while in realistic channel waveguide case, the entanglement reaches a maximum value of 0.33. This entanglement generation is the out turn of populations imbalance. In case of channel waveguide, after reaching a maximum value entanglement start decaying due to the decay rate of state populations.

Chapter 4

Entanglement sudden death

Entanglement sudden death (ESD) or early stage disentanglement [36, 25] is the phenomenon of degradation of a quantum correlation to zero in a finite time due to the presence of even a very weak dissipative environment. This dissipation attacks the entanglement, the fundamental source of quantum information. In this chapter ESD is investigated for different initial states and later on entanglement rebirth/revival is also observed to estimate the dark period for both geometries.

4.1 Entanglement sudden death and revival

In this section, different initial states are considered and their entanglement dynamics are evaluated.

4.1.1 Entangled State

Consider a non-maximally entangled initial state $|\Psi\rangle$,

$$|\Psi\rangle = \sqrt{1-a}|0\rangle + \sqrt{a}|3\rangle, \quad (4.1)$$

where $|0\rangle$ and $|3\rangle$ correspond to the ground and excited state respectively. The parameter a decides the degree of entanglement between ground and excited states. The variation of concurrence for the initial entangled state

$|\Psi\rangle$ is shown in Fig. 4.1 for both geometries. For $t = 0$, Eq. (2.33) reduces to $C_1(0) = 2\sqrt{a(1-a)}$. There is no entanglement for independently radiating a two-level system ($\Gamma = 0$). Hence, by using the condition $C_1(t) = 0$, death time of entanglement can be found as

$$T_d \simeq \frac{1}{\gamma} \ln \left(\frac{a}{a - \sqrt{a(1-a)}} \right). \quad (4.2)$$

It is evident from Eq. (4.2) that the disentanglement of qubits occurs for $a > 1/2$. Entanglement decays earlier and regenerates at later times due to a substantial population of symmetric and antisymmetric terms.

$$T_r \simeq \frac{k}{\gamma_{12}} \ln \left(\frac{4\gamma}{\sqrt{a}(\gamma - \gamma_{12})} \right). \quad (4.3)$$

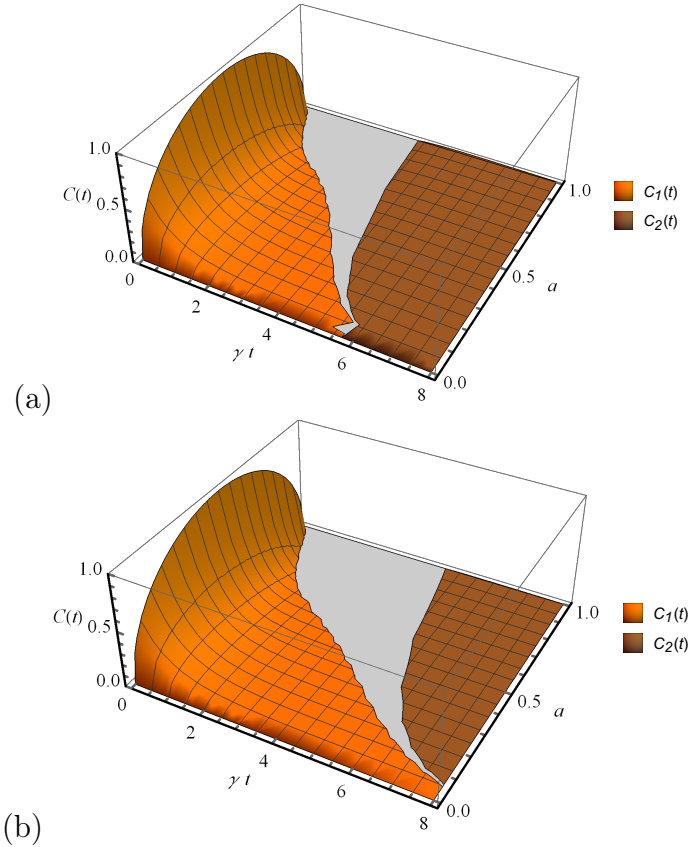


Figure 4.1: (Color online) Variation of $C(t)$ for initial entangled state $|\Psi\rangle$ at $d \simeq h$ for (a) cylinder and (b) channel.

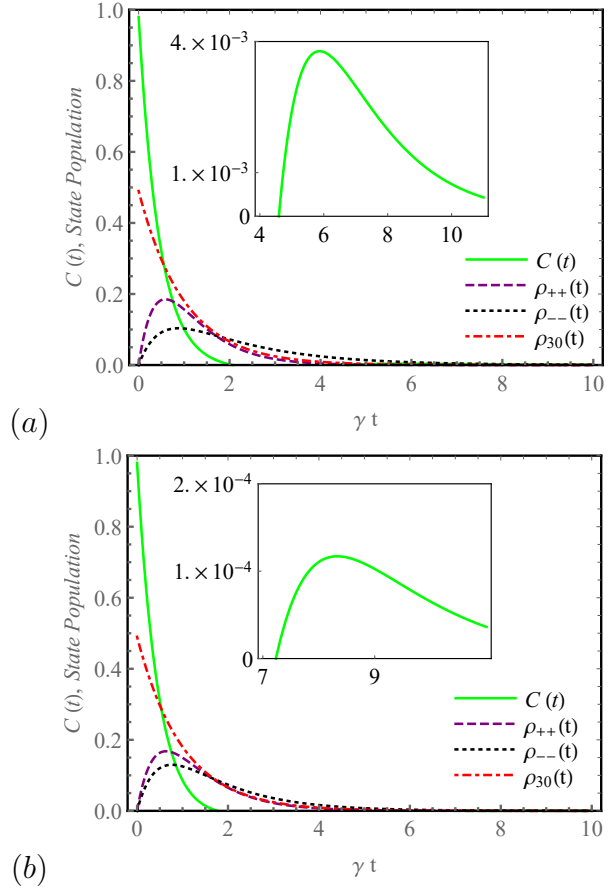


Figure 4.2: (Color online) Variation of $C(t)$ for initial entangled state $|\Psi\rangle$ at $a = 3/5$ and $d \simeq 5h/2$ for (a) cylinder and (b) channel

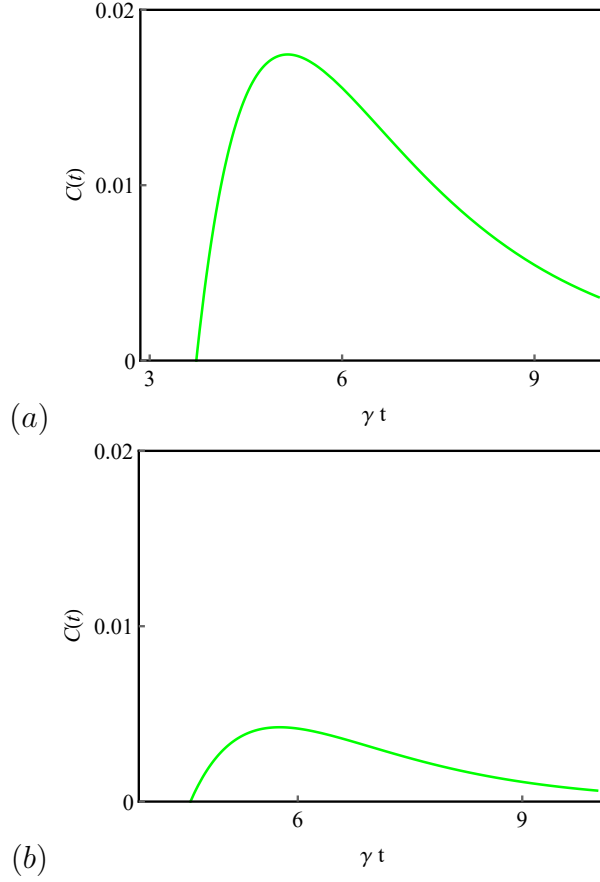


Figure 4.3: (Color online) Variation of $C(t)$ for limiting case with $d \simeq h$ for (a) cylinder and (b) channel

Recovery of entanglement is due to the collective damping term at $k \simeq 0.93$ and $k \simeq -1.29$ for cylinder and channel respectively when $a \simeq 3/5$ and $d \simeq h$. The dark period for cylindrical and channel geometry is estimated to be $2.41/\gamma$ and $3.46/\gamma$ respectively.

At large distance $d \simeq 5h/2$ between qubits, disentanglement occurs at $1.69/\gamma$ for both cylinder and channel while the regeneration of entanglement occurs at $4.6/\gamma$ and $7.25/\gamma$, respectively (see Fig. 4.2). At this separation both geometries experience a larger dark period ($2.91/\gamma$ for cylinder and $5.56/\gamma$ for channel) due to the instability of collective damping term with qubits separation. For a limiting case $a = 1$, Eq. (4.1) reduces to unentangled state

$|\Psi\rangle = |3\rangle$. Therefore density matrix elements reduces to

$$\begin{aligned}\rho_{33}(t) &= e^{-2\gamma t}, \\ \rho_{\pm\pm}(t) &= \frac{\gamma \pm \gamma_{12}}{\gamma \mp \gamma_{12}} e^{-(\gamma \pm \gamma_{12})t} - e^{-2\gamma t}.\end{aligned}\tag{4.4}$$

It can be grasped that entanglement will not appear for a limiting case but entanglement generates at a later time (caused by $C_2(t)$) due to an imbalance of symmetric and antisymmetric populations (see Fig. 4.3).

4.1.2 Mixed state

Consider a two-qubit system to be initially prepared in states of two spin 1/2 particles that are diagonal in the so-called Bell basis [37]. Initial density matrix is given as

$$\rho(0) = c \begin{pmatrix} s & 0 & 0 & 0 \\ 0 & 2 & 0 & 0 \\ 0 & 0 & 0 & 0 \\ 0 & 0 & 0 & v \end{pmatrix},\tag{4.5}$$

where $c = 1/3$ and $v = 1 - s$. Fig. 4.4 represents the variation of concurrence of initially mixed state at $d \simeq 5h/2$.

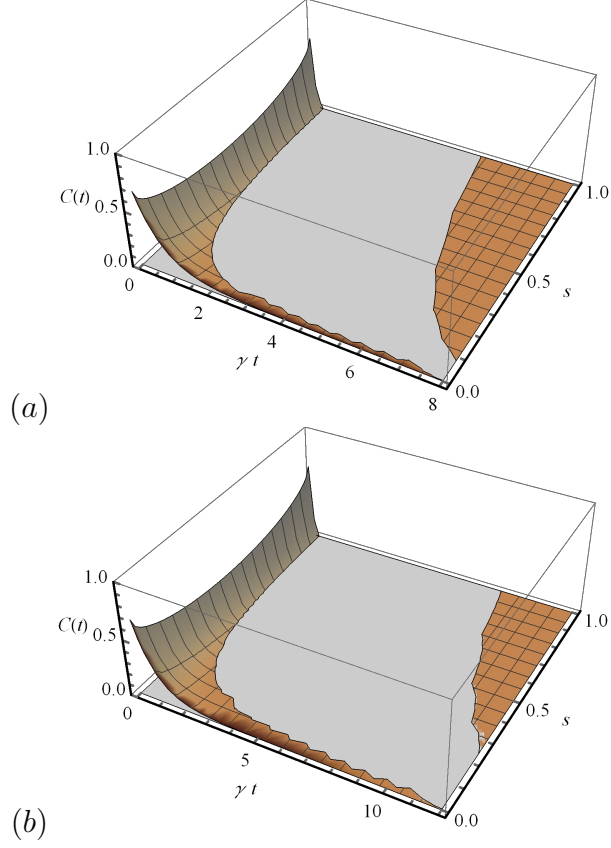


Figure 4.4: (Color online) Variation of $C(t)$ for mixed state $|\Psi\rangle$ at $d \simeq 5h/2$ for (a) cylinder and (b) channel.

In cylindrical geometry, qubits disentangled prior to the channel at $s \simeq 3/5$. At later times revival of entanglement occurs at $5.82/\gamma$ and $9.95/\gamma$ for cylinder and channel respectively. This leads to a less dark period of earlier as compared to the former geometry considering the variation of collective damping term with geometries.

4.1.3 Werner State

We suppose the initial Werner state [38] as

$$|\Psi_i\rangle = (1 - w)\frac{\mathbb{I}}{4} + w|+\rangle\langle+|, \quad (4.6)$$

where I denotes the identity matrix and parameter w determines the degree of entanglement. When the separation of qubits is kept approximately $5h/2$, then it can be seen that concurrence goes to zero at first and then revives at later times (see Fig. 4.5).

It is evaluated that ESD for cylinder occurs a little earlier as compared to channel for $w = 0.6$. Whereas entanglement revives approximately at $4/\gamma$ and $7.7/\gamma$ for cylinder and channel respectively. This eventually results in lesser dark period of cylindrical geometry as compared to the channel which is analogous to the trend of previously examined states.

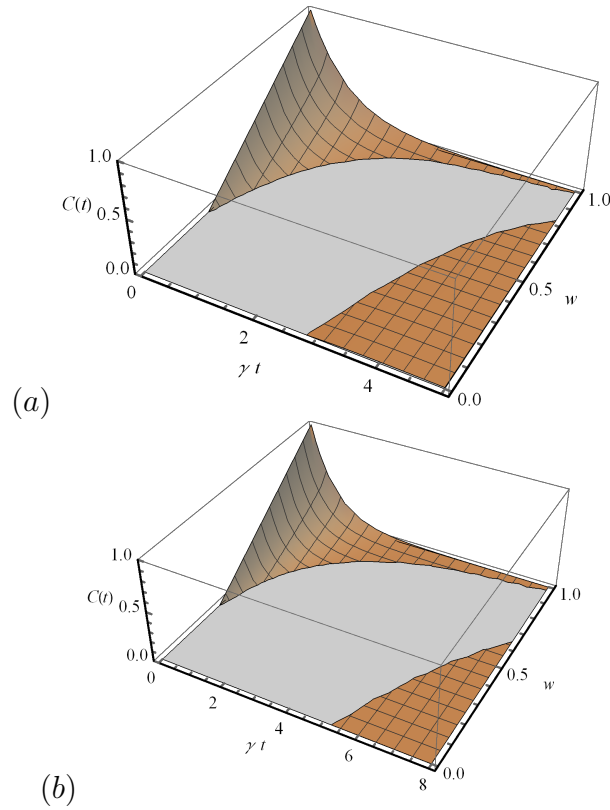


Figure 4.5: (Color online) Variation of $C(t)$ for initial state $|\Psi_i\rangle$ at $d \simeq 5h/2$ for (a) cylinder and (b) channel.

4.1.4 Maximally non local mixed state

The depiction of maximally nonlocal mixed states (MNMS) [39] for two photon coherence is given by initial density matrix as

$$\rho(0)^{\text{MNMS}} = \frac{1}{2} \begin{pmatrix} 1 & 0 & 0 & p \\ 0 & 0 & 0 & 0 \\ 0 & 0 & 0 & 0 \\ p & 0 & 0 & 1 \end{pmatrix}, \quad (4.7)$$

where $0 < p \leq 1$. Fig. 4.6 demonstrates the entanglement fluctuation of two-photon coherence MNMS for different values of initial coherence p . Sensitivity of entanglement dynamics with respect to initial amount of coherence is examined. Inset shows the revival of entanglement at later times for $d \simeq 5h/2$. Entanglement death time can be found by condition $C_1(t) = 0$ as

$$T_d \simeq \frac{1}{\gamma} \ln \left(\frac{1}{1-p} \right). \quad (4.8)$$

Disentanglement occurs at approximately $4.6/\gamma$ for both geometries but entanglement regenerates at $5.05/\gamma$ and $7.75/\gamma$ for cylinder and channel respectively for $p = 1$. For this value of initial coherence, cylinder and channel sustain a dark period of approximately $0.45/\gamma$ and $3.15/\gamma$ respectively. It can be perceived from Fig. 4.6 that concurrence with greater value of p decays to zero at later times as compared to the one with smaller value of p . Thus it can be concluded that the death time of entanglement is influenced by the initial coherence.

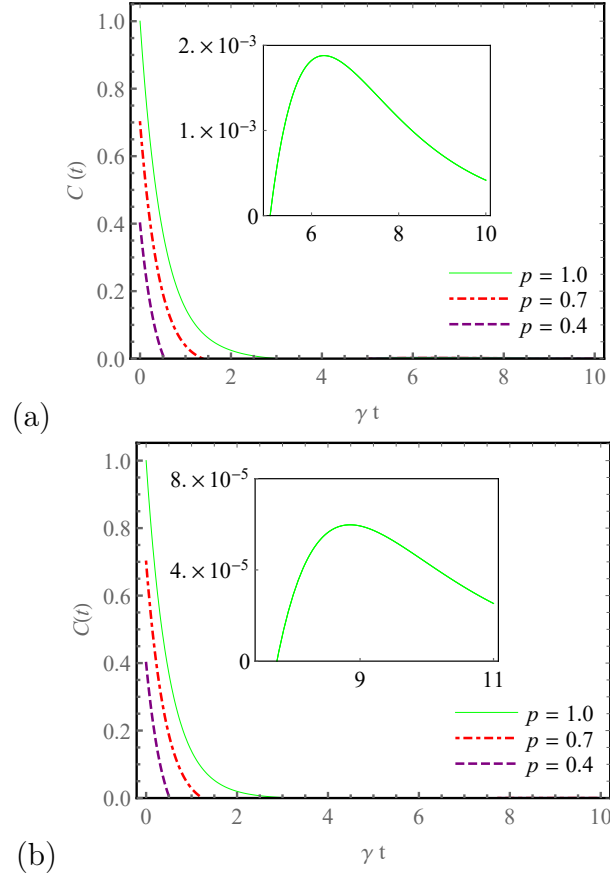


Figure 4.6: (Color online) Variation of a concurrence as function of dimensionless time parameter (γt) for two photon coherence MNMSs at $d \simeq 5h/2$ for (a) cylinder and (b) channel.

Entanglement rebirth comes earlier and is more consequential in cylindrical geometry as compared to the channel due to the collective damping term.

4.1.5 Maximally entangled mixed state

Maximally entangled mixed states (MEMSs) [40, 41] are the class of X-states that have the highest degree of entanglement. MEMSs for two-photon coherence are illustrated as

$$\rho(0)^{MEMS} = \begin{pmatrix} k(p) & 0 & 0 & p/2 \\ 0 & 1 - 2k(p) & 0 & 0 \\ 0 & 0 & 0 & 0 \\ p/2 & 0 & 0 & k(p) \end{pmatrix}, \quad (4.9)$$

where $k(p) = 1/3$ if $p < 2/3$ and $k(p) = p/2$ if $2/3 \leq p \leq 1$. Fig. 4.7 indicates the entanglement fluctuation of two-photon coherence MEMS for different initial coherence p . Inset in Fig. 4.7 shows the regeneration of entanglement at later times for $d = 5h/2$ (same as done in the case of MNMSs). By utilizing condition $C_1(t) = 0$ entanglement death time is appeared as

$$T_d \simeq \frac{1}{\gamma} \ln \left(\frac{2k}{1-p} \right). \quad (4.10)$$

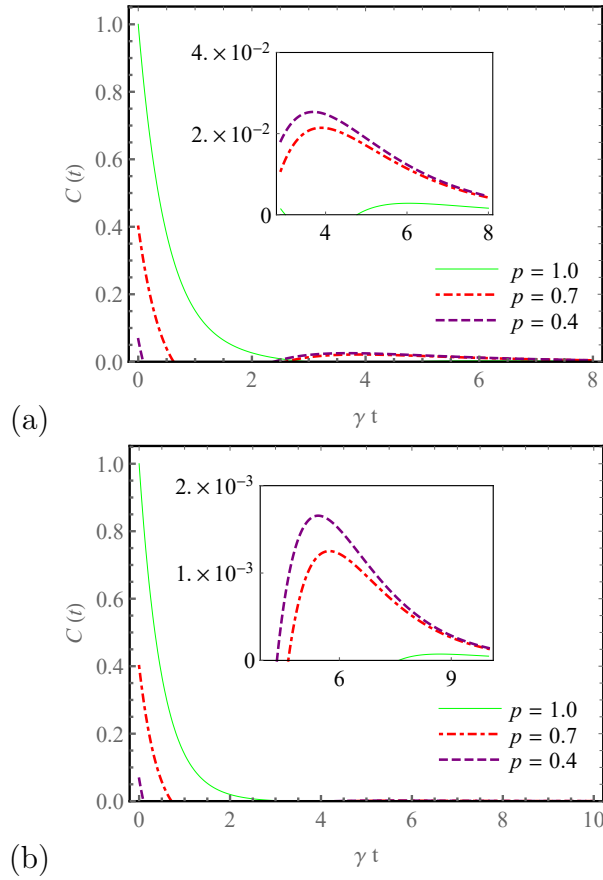


Figure 4.7: (Color online) Variation of a concurrence as function of dimensionless time parameter (γt) for two photon coherence MEMSs at $d \simeq 5h/2$ for (a) cylinder (b) channel.

Entanglement death and regeneration are observed for all values of p . Disentanglement occurs at $0.85/\gamma$ for both geometries while regenerates at $2.6/\gamma$

and $4.6/\gamma$ for cylinder and channel respectively at $p = 0.7$. For this value of initial coherence, the cylinder and channel go through a dark period of approximately $1.75/\gamma$ and $3.8/\gamma$ respectively. It can be observed that the behavior of entanglement is influenced by the amount of initial coherence (also observed in MNMS). The rebirth of entanglement is noticed as more remarkable in cylindrical geometry for all values of p .

4.2 Superdense coding

Superdense coding is an application of entanglement. Consider that the sender (Alice) and receiver (Bob) share qubits in the arbitrary entangled state ρ_{ab} . Alice encodes a message by performing Unitary operations U_k on a d -dimensional quantum system with a prior probability p_k on her qubit. After receiving, Bob will do a joint measurement operation to get the message (Fig. 4.8). The set of mutually orthogonal unitary transformations is necessary for

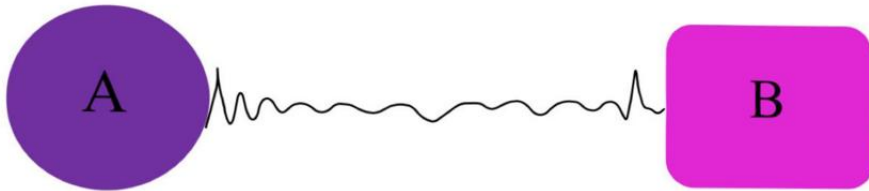


Figure 4.8: (Color online) Schematic representation of information transfer between sender and receiver.

this purpose. These unitary transformations for two qubits are represented as [42], $U_{00} |q\rangle = |q\rangle$, $U_{01} |q\rangle = |q + 1(\text{mod}2)\rangle$, $U_{10} |q\rangle = e^{i\pi q} |q\rangle$ and $U_{11} |q\rangle = e^{i\pi q} |q + 1(\text{mod}2)\rangle$. Thus Holevo bound gives the maximum possible amount of information that can be transferred as [43]

$$\chi = S(\rho'_{ab}) - \sum_k p_k S(\rho), \quad (4.11)$$

where $\rho'_{ab} = \sum p_k (U_k \otimes I_d) \rho_{ab} (U_k \otimes I_d)^\dagger$ and $S(\rho) = -\text{Tr}(\rho \log_d \rho)$ is the von Neumann entropy. The von Neumann entropy remains invariant un-

der any Unitary transformations hence superdense coding capacity χ can be redescrbed as [44, 45]

$$\chi = S(\rho'_{ab}) - S(\rho_{ab}). \quad (4.12)$$

For validation of dense coding capacity, χ must be greater than one, or else dense coding is not valid. The states for which dense coding capacity approaches its optimal value (χ tends to be 2) are useful in quantum communication. Different initial states are considered to analyze the variation of super-dense coding capacity.

4.2.1 Entangled state

Consider an entangled state as Eq. (4.1) to check the validity of dense coding capacity χ . It is noticed that the for maximally entangled state $a = 0.5$, dense coding capacity attains its maximum value $\chi = 2$. Maximum possible value varies for each probability amplitude a .

The χ decreases with decrease in degree of entanglement. From all the values of probability amplitudes, minimum capacity is observed for $a = 0.9$, which is the least entangled state of all. Moreover, it is observed that the dense coding is valid for more time in case of cylindrical waveguide as compared to the V-shaped channel (see insets of Fig. 4.9).

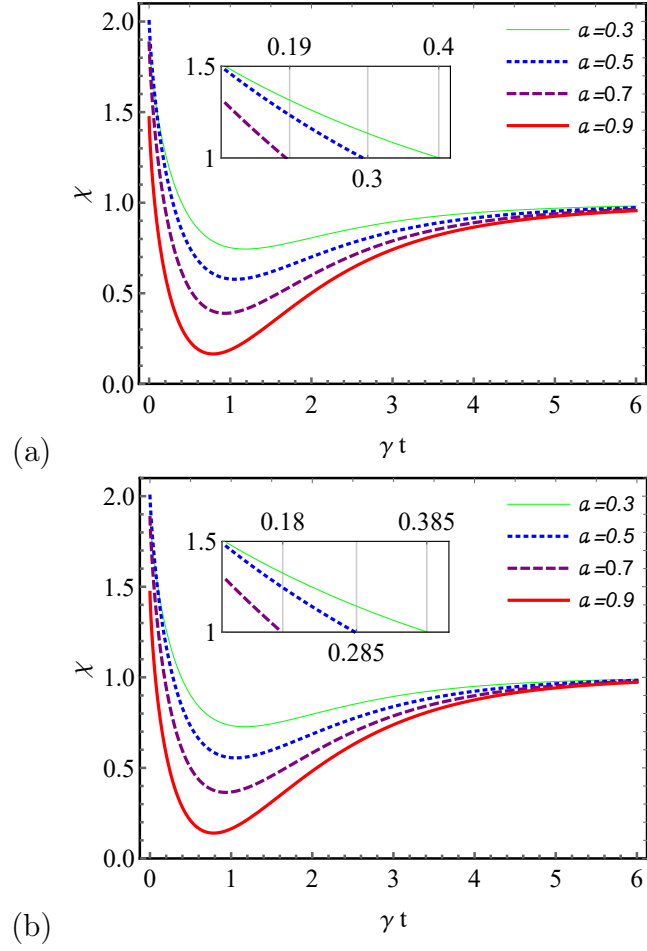


Figure 4.9: (Color online) Time variation of a χ for entangled state at $d \simeq 5h/2$ for (a) cylinder (b) channel.

4.2.2 Werner state

Consider an initial state as given in Eq. (4.6) to examine the validity of dense coding capacity.

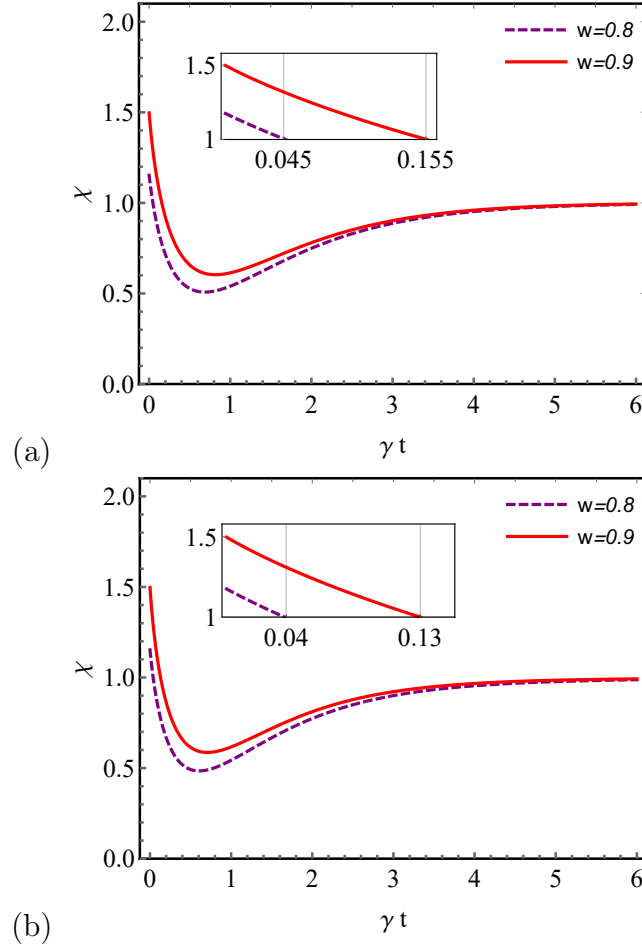


Figure 4.10: (Color online) Time variation of a χ for werner state at $d \simeq 5h/2$ for (a) cylinder (b) channel.

It is seen that the value of dense coding capacity decreases as the probability amplitude decreases due to the change in degree of entanglement. Moreover, the trend of previous state is also valid here that the optimal time of coding capacity is greater for cylindrical geometry as compared to V-shaped channel (see Fig. 4.10). The state with greater value of dense coding capacity has

a greater optimal time as compared to the one with smaller value of coding capacity. It proves the significance of more entangled state for quantum computation.

4.2.3 Maximally non-local mixed state

Consider MNMS as Eq. (4.7), the evolution of dense coding capacity is plotted for this state in Fig. 4.11. It is seen that the χ is maximum for initial coherence $p = 1$ and as the p decrease so does the coding capacity. The optimal time of dense coding capacity is seemed to be greater for cylindrical waveguide as compared to the V-shaped channel, the same as observed in earlier case. It is also worth noting that the curve with highest possible χ has a greater optimal time as compared to others. The coupling parameters oscillate with the plasmonic wavelength λ_{pl} as they are the functions of d . The influence of coherent and non-coherent terms in master equation changes with the qubit-qubit separation making the cylindrical geometry a significant one at the given specific d . The greater optimal time makes the state beneficial for quantum information technology.

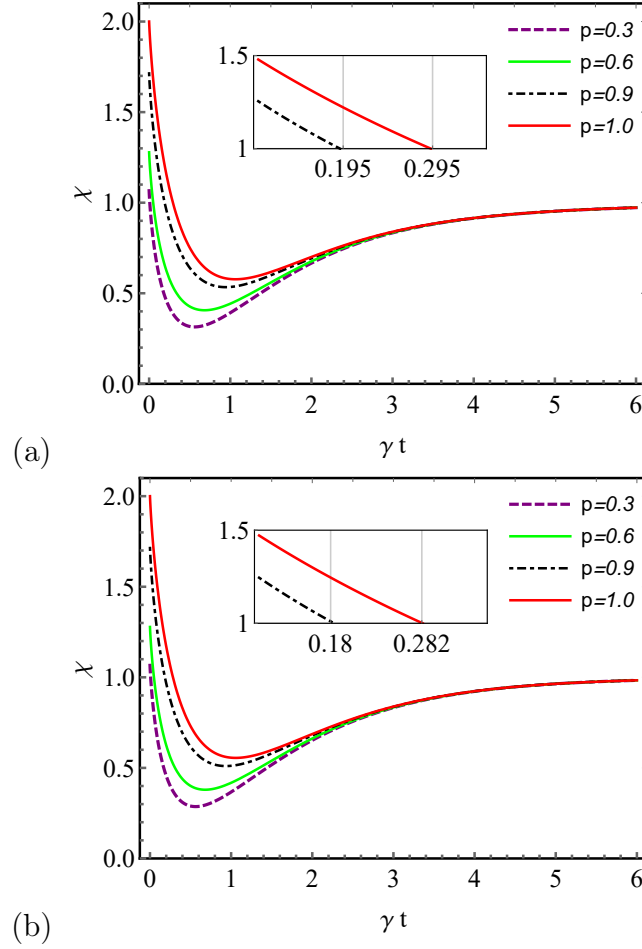


Figure 4.11: (Color online) Time variation of a χ for MNMS at $d \simeq 5h/2$ for (a) cylinder (b) channel.

4.2.4 Maximally entangled mixed state

To investigate the variation of superdense coding capacity in maximally entangled mixed state, consider a initial density matrix as Eq. (4.9). From Fig. 4.12 it is clear that MEMS has maximum possible value of χ . It is also noticed that the previous trend is also valid for MEMS. The cylindrical waveguide has the greater optimal time for dense coding as compared to the V-shaped channel.

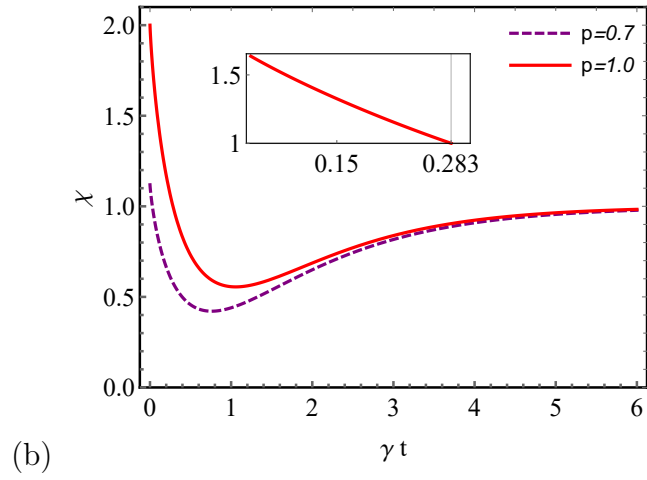
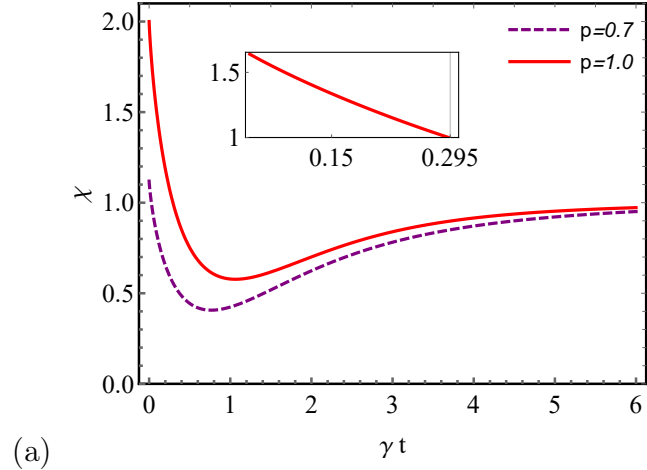


Figure 4.12: (Color online) Time variation of a χ for MEMS at $d \simeq 5h/2$ for (a) cylinder (b) channel.

Chapter 5

Result and discussion

The entanglement dynamics of two two-level system mediated by plasmonic waveguides and separated by a horizontal distance d are investigated. A master equation approach for two qubits is implemented to determine coherent and dissipative terms. In chapter 3, the entanglement generation of two qubits is studied. It is observed that the initially unentangled systems start getting entangled with time. This is due to the imbalance of state populations. The ideal PW and realistic PW are analyzed and it is seen that for ideal case, concurrence reaches upto the value of $C = 0.5$ while in case of realistic channel PW, entanglement reaches to the maximum value of $C = 0.33$, then decay to zero exponentially. For the realistic channel, state populations have finite decay rates therefore entanglement decay to zero. Furthermore, in chapter 4, sudden decay of entanglement of two qubit quantum system is investigated for channel and cylindrical geometries. The relationship of entanglement dynamics with the dissipative character of the two-qubit system is observed. The time of ESD and entanglement rebirth is evaluated for different initial states to estimate the dark period for both geometries. It is magnificent to see that in MEMSs entanglement regeneration is observed for all values of initial coherence. It is concluded that entanglement revival is more considerable for the cylindrical geometry as compared to the channel in the wake of the collective damping term. Lastly, SDC

is examined for different initial states, it is seen that maximally entangled state reaches maximum possible value of χ . Furthermore, it is observed that the optimal time of dense coding capacity is greater for cylindrical geometry as compared to V-shaped channel at a specific qubit-qubit separation. This makes the easier experimental realization of waveguide geometries for quantum communication and quantum information technology.

Bibliography

- [1] Kragh H. Max Planck: the reluctant revolutionary. *Physics World*. 2000;13(12):31.
- [2] Olszewski S. The Bohr model of the hydrogen atom revisited. *Reviews in Theoretical Science*. 2016;4(4):336-52.
- [3] Evans RD. Compton effect. Springer; 1958.
- [4] Granata V. The Davisson–Germer experiment. 2020:15-1.
- [5] Born M, Heisenberg W, Jordan P. On quantum mechanics II. *Z Phys*. 1926;35(8-9):557-615.
- [6] Przibram K, Schrödinger E, Einstein A, Lorentz HA, Planck M. Letters on wave mechanics. Vision; 1967.
- [7] Gieres F. Mathematical surprises and Dirac’s formalism in quantum mechanics. *Reports on Progress in Physics*. 2000;63(12):1893.
- [8] Bell JS. On the einstein podolsky rosen paradox. *Physics Physique Fizika*. 1964;1(3):195.
- [9] Kocher CA, Commins ED. Polarization correlation of photons emitted in an atomic cascade. *Physical Review Letters*. 1967;18(15):575.
- [10] Rempe G, Walther H, Klein N. Observation of quantum collapse and revival in a one-atom maser. *Physical review letters*. 1987;58(4):353.

- [11] Bennett CH, Brassard G. Quantum cryptography: Public key distribution and coin tossing. arXiv preprint arXiv:200306557. 2020.
- [12] Fuchs CA, Gisin N, Griffiths RB, Niu CS, Peres A. Optimal eavesdropping in quantum cryptography. I. Information bound and optimal strategy. *Physical Review A*. 1997;56(2):1163.
- [13] Zeitler CK, Chapman JC, Chitambar E, Kwiat PG. Entanglement verification of hyperentangled photon pairs. *Physical Review Applied*. 2022;18(5):054025.
- [14] Schumacher B. Quantum coding. *Physical Review A*. 1995;51(4):2738.
- [15] Mosseri R, Dandoloff R. Geometry of entangled states, Bloch spheres and Hopf fibrations. *Journal of Physics A: Mathematical and General*. 2001;34(47):10243.
- [16] Deffner S, Campbell S. Quantum speed limits: from Heisenberg's uncertainty principle to optimal quantum control. *Journal of Physics A: Mathematical and Theoretical*. 2017;50(45):453001.
- [17] Mintert F, Carvalho AR, Kuš M, Buchleitner A. Measures and dynamics of entangled states. *Physics Reports*. 2005;415(4):207-59.
- [18] Gisin N, Bechmann-Pasquinucci H. Bell inequality, Bell states and maximally entangled states for n qubits. *Physics Letters A*. 1998;246(1-2):1-6.
- [19] Blum K. *Density matrix theory and applications*. vol. 64. Springer Science & Business Media; 2012.
- [20] Zhang C, Wang G, Ying M. Discrimination between pure states and mixed states. *Physical Review A*. 2007;75(6):062306.
- [21] Martin-Cano D, González-Tudela A, Martín-Moreno L, García-Vidal F, Tejedor C, Moreno E. Dissipation-driven generation of two-qubit

- entanglement mediated by plasmonic waveguides. *Physical Review B*. 2011;84(23):235306.
- [22] Wootters WK. Entanglement of formation of an arbitrary state of two qubits. *Physical Review Letters*. 1998;80(10):2245.
- [23] Viola L, Lloyd S. Dynamical suppression of decoherence in two-state quantum systems. *Physical Review A*. 1998;58(4):2733.
- [24] Diósi L. Progressive decoherence and total environmental disentanglement. *Irreversible Quantum Dynamics*. 2003:157-63.
- [25] Yu T, Eberly J. Sudden death of entanglement. *Science*. 2009;323(5914):598-601.
- [26] Simon C, Kempe J. Robustness of multiparty entanglement. *Physical Review A*. 2002;65(5):052327.
- [27] Dür W, Briegel HJ. Stability of macroscopic entanglement under decoherence. *Physical review letters*. 2004;92(18):180403.
- [28] Yu T, Eberly J. Phonon decoherence of quantum entanglement: Robust and fragile states. *Physical Review B*. 2002;66(19):193306.
- [29] Bowen G. Classical information capacity of superdense coding. *Physical Review A*. 2001;63(2):022302.
- [30] Bennett CH, Wiesner SJ. Communication via one-and two-particle operators on Einstein-Podolsky-Rosen states. *Physical review letters*. 1992;69(20):2881.
- [31] Dzsotjan D, Sørensen AS, Fleischhauer M. Quantum emitters coupled to surface plasmons of a nanowire: A Green's function approach. *Physical Review B*. 2010;82(7):075427.

- [32] Søndergaard T, Bozhevolnyi S. Surface plasmon polariton scattering by a small particle placed near a metal surface: An analytical study. *Physical Review B*. 2004;69(4):045422.
- [33] Søndergaard T, Tromborg B. General theory for spontaneous emission in active dielectric microstructures: Example of a fiber amplifier. *Physical Review A*. 2001;64(3):033812.
- [34] Jin J, Li J, Liu Y, Li XQ, Yan Y. Improved master equation approach to quantum transport: From Born to self-consistent Born approximation. *The Journal of chemical physics*. 2014;140(24).
- [35] Dicke RH. Coherence in spontaneous radiation processes. *Physical review*. 1954;93(1):99.
- [36] Yu T, Eberly J. Finite-time disentanglement via spontaneous emission. *Physical Review Letters*. 2004;93(14):140404.
- [37] Bennett CH, DiVincenzo DP, Smolin JA, Wootters WK. Mixed-state entanglement and quantum error correction. *Physical Review A*. 1996;54(5):3824.
- [38] Hiroshima T, Ishizaka S. Local and nonlocal properties of Werner states. *Physical Review A*. 2000;62(4):044302.
- [39] Batle J, Casas M. Nonlocality and entanglement in qubit systems. *Journal of Physics A: Mathematical and Theoretical*. 2011;44(44):445304.
- [40] Munro WJ, James DF, White AG, Kwiat PG. Maximizing the entanglement of two mixed qubits. *Physical Review A*. 2001;64(3):030302.
- [41] Ishizaka S, Hiroshima T. Maximally entangled mixed states under nonlocal unitary operations in two qubits. *Physical Review A*. 2000;62(2):022310.

- [42] Hiroshima T. Optimal dense coding with mixed state entanglement. *Journal of Physics A: Mathematical and General*. 2001;34(35):6907.
- [43] Holevo AS. Bounds for the quantity of information transmitted by a quantum communication channel. *Problemy Peredachi Informatsii*. 1973;9(3):3-11.
- [44] Li YQ, Li X, Jia XF, Yang GH. Quantum dense coding properties between two spatially separated atoms in free space. *International Journal of Theoretical Physics*. 2020;59:3378-86.
- [45] Xu HY, Yang GH. Quantum dense coding about a two-qubit Heisenberg XYZ model. *International Journal of Theoretical Physics*. 2017;56:2803-10.